Original Article

The protective role of cigarette smoking against Parkinson's disease via moderation of the interaction between iron deposition in the nigrostriatal pathway and clinical symptoms

Quanquan Gu[1#]^, Xiaocao Liu[1#], Qingze Zeng[1], Xiaojun Guan[1], Cheng Zhou[1], Tao Guo[1], Baorong Zhang[2], Minming Zhang[1]

[1]Department of Radiology, The Second Affiliated Hospital, Zhejiang University School of Medicine, Hangzhou, China; [2]Department of Neurology, The Second Affiliated Hospital, Zhejiang University School of Medicine, Hangzhou, China

Contributions: (I) Conception and design: Q Gu; (II) Administrative support: Q Gu, X Liu, Q Zeng; (III) Provision of study materials or patients: Q Gu, X Liu, X Guan, C Zhou, T Guo, B Zhang; (IV) Collection and assembly of data: Q Gu, X Liu, Q Zeng; (V) Data analysis and interpretation: Q Gu, X Liu, Q Zeng; (VI) Manuscript writing: All authors; (VII) Final approval of manuscript: All authors.

[#]The authors contributed equally to this work.

Correspondence to: Quanquan Gu. Department of Radiology, The Second Affiliated Hospital, Zhejiang University School of Medicine, 88 Jiefang Road, Hangzhou 310009, China. Email: zju_gqq@zju.edu.cn.

Background: Although cigarette smoking is a risk factor for multiple disorders, it has long been thought to protect against Parkinson's disease (PD). Quantitative susceptibility mapping (QSM) is a novel magnetic resonance imaging (MRI)-based technique for assessing iron accumulation *in vivo* that has been widely applied in PD studies. This study aimed to investigate how cigarette smoking affects clinical performance of PD using quantified iron deposition as a proxy for PD pathology.

Methods: In this observational study, we enrolled 35 male PD patients and 47 male healthy controls (HCs) and divided them into four groups. We performed an enhanced T2 star-weighted angiography (ESWAN) MRI sequence to measure the iron content of the nuclei within the nigrostriatal pathway. With the age and total intracranial volume (TIV) controlled as covariates, we performed inter-group comparisons of QSM values and moderation analyses for PD patients using smoking status and the smoking index (SI), respectively, as moderator variables.

Results: The 2-way multivariate analysis of covariance (MANCOVA) results showed higher QSM values in the left red nucleus (P=0.024) in PD patients compared with those in HCs, and in the bilateral globi pallidi [left/right (L/R): P=0.009/0.003], substantia nigra pars compacta (SNc; L/R: P=0.001/0.037), and right substantia nigra pars reticulata (SNr; P=0.002) in non-smokers compared with smokers, with no marked interaction effect between PD and smoking status observed when applying the Bonferroni adjustment for multiple comparisons. Using cigarette smoking status and the SI as separate moderator variables, the moderation was shown up by a significant interaction effect in a disordinal and double-edged form. In our results, smoking-moderated protection for PD movement deficits emerged when PD was progressed. Among the affected deep brain nuclei, the nuclei most moderated by the impact of cigarette smoking on the interaction between brain iron and PD symptoms were the thalamus [smoking status associated with the Unified Parkinson's Disease Rating Scale (UPDRS) total score, P=0.04 (L); rigidity, P=0.03 (L); SI associated with UPDRS-III, P (L/R) =0.049/0.0497; rigidity, P (L/R) =0.01/0.02; bradykinesia, P (L/R) =0.048/0.04], the right red nucleus (SI associated with rigidity, P=0.04; bradykinesia, P=0.02), and the left SNc [smoking

^ ORCID: 0000-0002-2723-2069.

status associated with the Hoehn and Yahr (H&Y) stage, P=0.01].

Conclusions: This was the first study investigating the impacts of current cigarette smoking on PD using quantified iron deposition. Our study confirmed the protective role of cigarette smoking against PD, consistent with the findings of previous studies. Furthermore, neuroprotection was present only when the PD pathology had progressed to a certain extent. In the interaction between iron deposition and clinical PD symptoms, our findings suggest that the thalamus, red nucleus, and SNc are likely to be the most affected nuclei moderated by cigarette smoking.

Keywords: Quantitative susceptibility mapping (QSM); magnetic resonance imaging (MRI); Parkinson's disease (PD); cigarette smoking; iron deposition

Submitted Nov 09, 2021. Accepted for publication Apr 06, 2022.
doi: 10.21037/qims-21-1090
View this article at: https://dx.doi.org/10.21037/qims-21-1090

Introduction

Parkinson's disease (PD) is characterized by neurodegeneration in the deep brain nuclei located in the nigrostriatal pathway (1), which can be reflected by changes in the iron deposition in these nuclei (2-5). Cigarette smoking has long been considered a health hazard linked to a variety of illnesses: it causes vascular complications and subclinical brain infarctions (6) by increasing oxidative stress, which deteriorates vascular function and promotes vascular remodeling in the brain (7). However, prior research has repeatedly revealed a strong reverse association between cigarette smoking and PD progression (8-11), in which smoking delays the onset of PD (12) and reduces the risk of PD by 41–58% (13). In contrast to non-smokers, most PD patients with a history of smoking have less severe motor symptoms, such as tremor (14) and levodopa-induced dyskinesia (15), but worse non-motor symptoms, including cognition, sleep disorders, and psychiatric disorders such as impulsive-compulsive behaviors (16-18). Some researchers have suggested that this reverse association is related to a pathophysiological rationale based on the imbalance between nicotinic cholinergic and dopaminergic neurotransmitter systems in the nigrostriatal pathway (19-21), but the exact mechanism is still unclear.

In consideration of previous studies, we aimed to demonstrate the impact of cigarette smoking on the interplay between PD progression and severity of clinical symptoms using quantified iron deposition as a proxy for PD pathology. We hypothesized that cigarette smoking rendered a positive impact on the interaction between iron deposition and PD symptoms by affecting key nodes within the nigrostriatal pathway. The quantitative susceptibility mapping (QSM) technique is a novel and robust magnetic resonance imaging (MRI) technique quantifying abnormal iron accumulation in the brain, which has been shown to align closely with the core pathology of PD (2-5). The QSM was used by our present study as a surrogate biomarker for PD pathology, with the aim to further the understanding of the protective role of cigarette smoking for PD. We present the following article in accordance with the STROBE reporting checklist (available at https://qims.amegroups.com/article/view/10.21037/qims-21-1090/rc).

Methods

Participants

We performed a case-control, observational study for patients diagnosed by the Department of Neurology at the Second Affiliated Hospital of Zhejiang University School of Medicine, from 1 August, 2014, to 1 December, 2018. The exclusion criteria included a self-reported history of neurological or psychiatric disease, previous drug or alcohol use, or traumatic brain injury. All enrolled participants were able to tolerate MRI scans and cooperatively complete all the scale tests. The study was conducted in accordance with the Declaration of Helsinki (as revised in 2013). The study was approved by the Ethical Review Board at Zhejiang University, and informed consent was provided by all participants. There were 227 patients with an initial diagnosis of PD, of which 122 were eventually diagnosed; of these, 35 patients with PD agreed to participate in the present study and were able to complete all the scale tests. The healthy controls (HCs; n=167) were recruited in and around Hangzhou City, including 66 males and 101 females, of which 45 males were

enrolled and able to tolerate MRI scans. Thus, before the study started, we enrolled a total of 35 patients with PD (aged 57.75±8.06 years) and 47 age-matched HCs (aged 60.77±6.69 years). The diagnosis of PD was made according to the UK Parkinson's Disease Society Brain Bank criteria (22). The patients had a longer than 12-hour withdrawal from medication before commencement of the study and were all off medication during the clinical battery assessment, which included the duration of disease, Hoehn and Yahr (H&Y) scale (23), Unified Parkinson's Disease Rating Scale (UPDRS) total score, including part III scores, the tremor, rigidity, bradykinesia, and axial scores (24), the Mini-Mental State Examination (MMSE) (25), and cigarette consumption [e.g., smoking index (SI) (26)]. The duration of disease was defined as the time from when a patient became self-conscious of exhibiting parkinsonian signs.

To eliminate the confusing effect of smoking cessation, only continuous and current smokers were enrolled in the present study. As male smokers account for the vast majority of smokers in China (52.9% of men and 2.4% of women are current smokers in China) (27), we recruited exclusively male participants. We calculated the SI according to the formula proposed in a study by Indrayan *et al.* (26), as follows:

$$S=\left(3-\frac{a}{15}\right)\frac{1}{2}\sqrt{\sum p_i n_i x_i-0.5}-y;\ \text{for } S\geq 0,\ \text{and } \sum p_i n_i x_i\geq 0.5;$$

otherwise, zero (use a=30 for a>30); where a is the age at the start of smoking, p_i is the proportion of smoke inhaled in the case of passive smoking (or adjustment for filter cigarettes or for other forms of smoking), x_i is the number of cigarettes smoked for n_i years, and y is the number of years elapsed since cessation by ex-smokers, which measures the present burden in an absolute sense and not the risk of smoking-related diseases (26). The non-smoking participants were defined as those who had smoked less than one-half of a cigarette-year in a lifetime (26).

We divided the participants into 4 subgroups based on smoking status (yes/no): 24 cases in the HC non-smoker subgroup (ns-HC, aged 60.66±6.25 years), 17 in the PD non-smoker subgroup (ns-PD, aged 57.71±8.65 years), 23 in the HC smoker subgroup (s-HC, aged 60.88±7.27 years), and 18 in the PD smoker subgroup (s-PD, aged 57.79±7.70 years). In total, 35 PD patients and 47 HCs were recruited into the present study, of which 41 participants were smokers and 41were non-smokers. We performed the normality test for all the epidemiological data using the Kolmogorov-Smirnov test. During the inter-group comparisons, we used one-way analysis of variance (ANOVA) and the Student's *t*-test for data that were normally distributed; we used the non-parametric method for data that were not normally distributed. The statistical significance was set at P <0.05. The participants' profiles are detailed in *Table 1*.

MRI acquisition and QSM data processing

All participants were scanned using an 8-channel head/neck coil on a 3.0 Tesla MRI scanner (GE Discovery 750, GE Healthcare, Milwaukee, WI, USA). The head was stabilized with restraining foam pads during the scanning, and earplugs were provided to decrease the noise. A 3D-multi-echo gradient recalled echo (GRE) sequence was used to acquire enhanced susceptibility-weighted angiography (ESWAN) images, and the imaging parameters were as follows: repetition time =33.7 ms; 1st echo time/spacing/8th echo time =4.556 ms/3.648 ms/30.092 ms; flip angle =20 degrees; field of view =240×240 mm^2; matrix =416×384; slice thickness =2 mm. All the images obtained from the participants were carefully checked after scanning. Image quality was checked by 2 experienced radiologists to make sure participants had no visible head movements.

Phase images were calculated on a computer cluster using the Susceptibility Tensor Imaging (STI) Suite v3.0 software package (https://people.eecs.berkeley.edu/chunlei.liu/software.html). First, the raw phase images were unwrapped using the Laplacian method based on the sine and cosine functions of the phase angle, and then the normalized phase images were calculated (28-30). Next, the background phase information was removed using the spherical-mean-value filtering (V-SHARP) method (29). After the background phase removal process, tissue susceptibilities were calculated using the Streaking Artifact Reduction for QSM (STAR-QSM) method (31,32). The mean magnetic susceptibility mapping of each individual brain was used as the susceptibility reference.

Region of interest determination

The tissue susceptibility of native subcortical nuclei in the bilateral substantia nigra pars compacta (SNc) and pars reticulata (SNr), red nuclei, putamen, caudates, globi pallidus, and thalami was determined (shown in *Figure 1*) (2). The specific methods were as follows: (I) the native QSM image was registered to a newly constructed QSM template derived from a cohort of aging brains, using Advanced Neuroimaging Tools-Symmetric Normalization (ANTs-

Table 1 Participant demographic information

Variable	HC		PD		F (t)	P value
	Non-smoker (ns-HC)	Smoking (s-HC)	Non-smoker (ns-PD)	Smoker (s-PD)		
Participants	24	23	17	18	–	0.82
Age (years)	60.66±6.25	60.88±7.27	57.71±8.65	57.79±7.70	1.12	0.35
Gender (male/female)	24/0	23/0	17/0	18/0	–	–
Duration	–	–	3.85±2.74	2.70±2.23	–	0.26†
MMSE	–	–	26.71±3.14	27.28±2.74	–	0.38†
UPDRS total	–	–	35.94±22.12	37.72±18.37	–0.26	0.80
UPDRS III	–	–	26.35±16.52	26.39±13.48	–0.01	0.99
Axial	–	–	4.53±2.74	4.67±3.16	–0.14	0.89
Rigidity	–	–	5.59±2.83	5.67±4.23	–	0.91†
Bradykinesia	–	–	11.12±7.85	11.89±6.57	0.05	0.75
Tremor	–	–	4.88±3.01	4.00±4.01	–	0.35†
Hoehn and Yahr (H&Y) stage	–	–	2.32±0.39	2.33±0.45	–	0.29†
Smoking index	–	15.21±6.76	–	12.09±13.34	–	0.03†*
TIV	1,555.90±198.97	1,560.24±104.59	1,536.24±139.90	1,563.75±102.70	0.12	0.95

†, the result is obtained by the Kolmogorov-Smirnov (K-S) nonparametric test; *, indicates a statistical significance with a threshold of P<0.05. PD, Parkinson's disease; HC, healthy control; MMSE, the Mini-Mental State Examination; UPDRS, Unified Parkinson Disease Rating Scale; UPDRS III, UPDRS Part III; TIV, total intracranial volume.

SyN) coregistration algorithms (33); (II) the labels covering the subcortical nuclei were defined in the QSM template; (III) the labels in the QSM template were then warped to the native QSM image space by inverting the transformation matrix calculated in the first step; (IV) manual refinement was performed to ensure segmentation precision using ITK-SNAP v3.2 software (http://www.itksnap.org). The regions of interest (ROIs) of each nucleus were extracted from all the slices of each participant where the nucleus could be found. A radiologist (with 5 years of experience in neuroimaging diagnosis) who was blind to the information of the participants, including disease condition and demographics, performed the ROI drawing twice. The ROIs of each participant were defined using the averaged masks of the repeatedly drawn ROIs. Finally, the mean tissue susceptibility of bilateral subcortical nuclei was calculated, indicating the iron content in each of the 14 nuclei.

Total intracranial volume (TIV) calculation

The structural images were preprocessed using the Computational Anatomy Toolbox 12 (CAT12, http://www.neuro.uni-jena.de/cat/) of the statistical parametric mapping 12 (SPM12) software on the Matrix Laboratory (MATLAB) platform (MathWorks Inc., Natick, MA, USA). Briefly, the brain 3D T1-weighted images were normalized to the Montreal Neurological Institute (MNI) 152 template and then segmented into gray matter, white matter, and cerebrospinal fluid (CSF). After that, the TIV of individuals was separately calculated.

QSM statistical analysis and moderation analysis

The statistical analyses were performed using the software SPSS 26.0 (IBM Corp., Armonk, NY, USA). An inter-group, one-way analysis of covariance (ANCOVA) test followed by pair-wise comparisons was performed to compare the QSM values across the groups, with age and TIV as covariates. Another 2-way multivariate analysis of covariance (MANCOVA) test (2-tailed) was then performed with the covariates of age and TIV set to eliminate the effects from them, in which the two factors were PD condition and cigarette smoking status (yes/no) and the dependent variables were QSM values of the ROIs, as

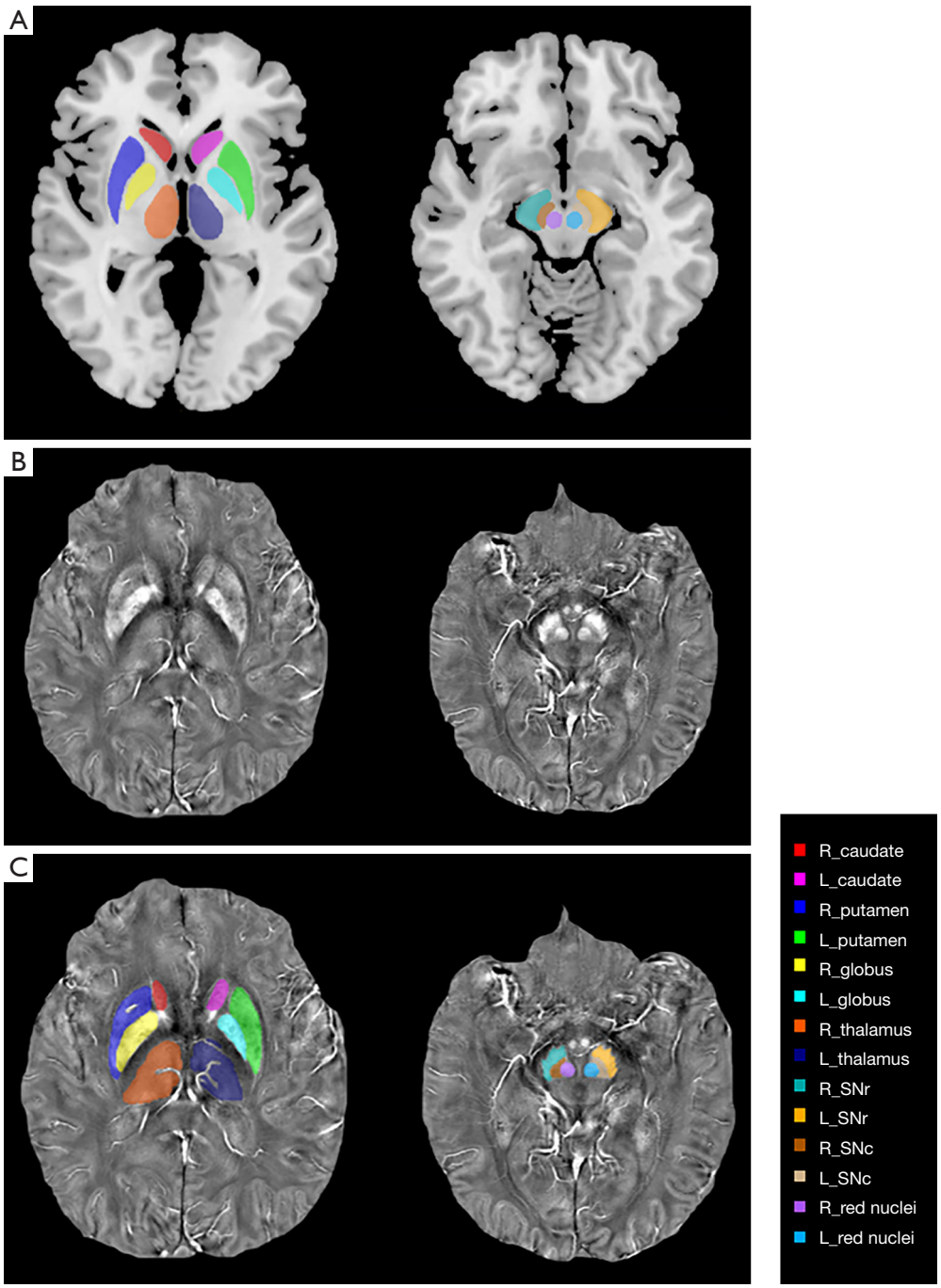

Figure 1 The ROIs of the deep brain nuclei. (A) The anatomical diagram of the 14 nuclei; the legend on the right indicates the various colors representing different nuclei; (B) the native QSM image used in this study; (C) final labels in the data analysis after manual revision. ROIs, regions of interest; QSM, quantitative susceptibility mapping.

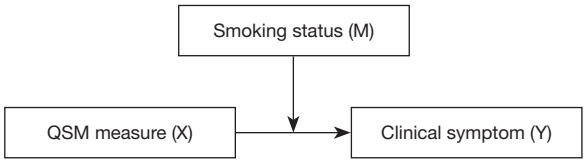

Figure 2 The model of moderation analysis. The moderation analysis was performed based on Model 1 in the PROCESS macro using SPSS statistical software (version 3.5 by Andrew Hayes, http://www.afhayes.com). According to this model of moderated multiple regression, for each PD patient, the outcome variable (labelled Y) was quantified clinical symptoms, the predictor or independent variable (labelled X) was a QSM measure derived from each ROI as defined in the Methods section, and the moderator variable (labelled M) was specified for smoking status (yes/no). PD, Parkinson's disease; QSM, quantitative susceptibility mapping; ROI, regions of interest.

previously mentioned. To further find out where the significance came from, post-hoc pairwise *t*-tests were used following the ANCOVA test. A significance level of P<0.05 was applied, with correction for multiple comparisons using the Bonferroni correction.

Moderation analysis for PD patients was performed via the PROCESS macro (Model 1) with covariates of ages and TIV in SPSS (34). The conceptual form of the moderated model is presented in *Figure 2*. For each moderation model, separate analyses for the moderator variables (labelled M) of smoking status (yes/no) and the SI were run, with outcome variables (labelled Y) as quantified scoring of clinical symptoms (including H&Y stage, disease duration, total and each part of UPDRS scores, targeted symptoms such as axial symptoms, tremor, rigidity, bradykinesia scores, and MMSE scores) and predictor variables (labelled X) as QSM values derived from the nuclei, as mentioned earlier in the description of ROI drawing. The difference in path coefficients with statistical significance (P<0.05) between the two groups was taken as proof of the moderation effect in this path (35). A 5,000 times bootstrapping procedure was used to test the significance of the differences at levels of moderator variables. The variables were all mean-centered for construction of products in the moderated regression model.

Results

We carefully matched for other possible confounding factors across the four subgroups, including the duration of the condition, general severity of the disease, state of movement, and cigarette smoking status. *Table 1* shows there were no significant inter-group differences in the demographic information.

QSM values

In the ANCOVA test, there was significant inter-group difference in the QSM values (F=1.573, P=0.022). In the following pair-wise comparisons, the difference was found to come from the right globus pallidus (ns-HC *vs.* s-PD, P=0.028), left red nucleus (ns-PD *vs.* s-HC, P=0.028), left SNc (ns-PD *vs.* s-HC, P=0.003) (*Table 2*, Figure S1). The MANCOVA test further studied the main and interaction effects of the variables. As shown in the results, on the smoking status, participants who did not smoke had significantly higher QSM values than those who smoked in ROIs of the bilateral globi pallidi (left: F=7.197, P=0.009; right: F=9.150, P=0.003), bilateral SNc (left: F=11.435, P=0.001; right: F=4.488, P=0.037), and right SNr (F=10.435, P=0.002). Besides, under the PD condition, the PD patients exhibited significantly higher QSM values than the HCs in the left red nucleus (F=5.327, P=0.024) (*Table 3*). However, the interactional effect between smoking and PD conditions was not significant (F=1.080, P=0.393). We provide the details of the susceptibility values of all deep brain nuclei (Table S1) and the ROIs with significant differences in QSM values across the four subgroups (Figure S2) in the Supplementary material section. The results of inter-group QSM value comparisons were also shown with age, TIV, and disease duration as covariates (please refer to Tables S2,S3).

Moderation analysis

By controlling the impacts of TIV and age, we found the statistically significant moderating effect of cigarette smoking status on the interactions of the QSM values of the left thalamus and the UPDRS total scores [B=–2,628.72, 95% confidence interval (CI): –5,199.90 to –57.53; t=–2.09; P=0.04) and rigidity scores (B=–823.74, 95% CI: –1,366.68 to –280.80; t=–3.10; P=0.03), of the left SNc and H&Y stages (B=29.27, 95% CI: 7.21 to 51.32; t=2.71; P=0.01) in patients with PD (detailed in *Table 4*), with a graphic presentation illustrated in *Figure 3*. Likewise, the statistically significant moderating effect of the SI on the interactions of the QSM values of the bilateral thalamus and the UPDRS III scores (left: B=–127.77, 95% CI: –255.11 to

Table 2 The ROIs with significant differences in QSM values (ppm) across groups

Source	Main effect		Pairwise comparison					
	F	P value (*)	Group (I-J)	Mean difference (I-J)	SE	P' value (*)	95% CI	
							Lower	Upper
R_GP	3.503	0.019*	ns-HC-ns-PD	0.004	0.008	1.000	−0.016	0.025
			ns-HC-s-HC	0.015	0.007	0.219	−0.004	0.033
			ns-HC-s-PD	0.022	0.007	0.028*	0.002	0.042
			ns-PD-s-HC	0.010	0.008	1.000	−0.010	0.031
			ns-PD-s-PD	0.017	0.008	0.204	−0.004	0.039
			s-HC-s-PD	0.007	0.008	1.000	−0.013	0.027
L_RN	2.925	0.039*	ns-HC-ns-PD	−0.015	0.007	0.215	−0.033	0.004
			ns-HC-s-HC	0.006	0.006	1.000	−0.011	0.022
			ns-HC-s-PD	−0.002	0.007	1.000	−0.020	0.016
			ns-PD-s-HC	0.020	0.007	0.028*	0.001	0.039
			ns-PD-s-PD	0.012	0.007	0.554	−0.007	0.032
			s-HC-s-PD	−0.008	0.007	1.000	−0.026	0.010
L_SNc	4.809	0.004*	ns-HC-ns-PD	−0.009	0.005	0.507	−0.023	0.005
			ns-HC-s-HC	0.010	0.005	0.237	−0.003	0.022
			ns-HC-s-PD	0.005	0.005	1.000	−0.008	0.019
			ns-PD-s-HC	0.019	0.005	0.003*	0.005	0.033
			ns-PD-s-PD	0.014	0.005	0.057	0.000	0.029
			s-HC-s-PD	−0.004	0.005	1.000	−0.018	0.009

I-J means the two groups for comparison. Multiple pairwise comparisons were corrected by Bonferroni method, with a pre-adjusted significance (*) level at P'<0.05. QSM, quantitative susceptibility mapping; GP, globus pallidum; RN, red nucleus; SNc, substantia nigra pars compacta; SNr, substantia nigra pars reticulata; SE, standard error; CI, confidence interval.

Table 3 Two-way MANCOVA and pairwise comparisons in QSM values (ppm) across groups

Source	Mean square	F	Partial eta square	Pairwise comparison					
				Group (I > J)	Mean difference (I-J)	SE	P' value (*)	95% CI	
								Lower	Upper
PD status									
L_RN	0.002	5.327	0.065	PD > HC	0.011	0.005	0.024*	0.002	0.021
Smoking status									
R_GP	0.005	9.150	0.107	Non-smoker > Smoker	0.016	0.005	0.003*	0.005	0.027
L_GP	0.004	7.197	0.087		0.015	0.005	0.009*	0.004	0.026
R_SNc	0.001	4.488	0.056		0.008	0.004	0.037*	0.000	0.015
L_SNc	0.003	11.435	0.131		0.012	0.004	0.001*	0.005	0.019
R_SNr	0.005	10.435	0.121		0.015	0.005	0.002*	0.006	0.025

The threshold of pre-adjusted significance (*) was regarded as P'<0.05 corrected by Bonferroni method. MANCOVA, multivariate analysis of covariance; QSM, quantitative susceptibility mapping; PD, Parkinson's disease; GP, globus pallidum; RN, red nucleus; SNc, substantia nigra compacta; SNr, substantia nigra pars reticulata; CI, confidence interval.

Table 4 Outputs of moderation analysis for PD patients (moderator variable: smoking status)

Source	B	SE	t	P value	95% CI	
					Lower	Upper
Panel 1						
Main moderation analysis-UPDRS total score						
Constant	−71.24	54.76	−1.30	0.20	−183.24	40.75
Left thalamus QSM	519.51	749.54	0.69	0.49	−1,013.50	2052.53
Smoking status	1.06	6.12	0.17	0.86	−11.45	13.57
Left thalamus QSM × smoking status	−2,628.72	1,257.13	−2.09	0.04*	−5,199.90	−57.53
Age	1.29	0.49	2.62	0.01	0.28	2.29
TIV	0.02	0.03	0.79	0.43	-0.03	0.08
Conditional effect of moderator						
Smoking status						
No	1,871.43	1,027.39	1.82	0.08	−229.87	3,972.72
Yes	−757.29	929.04	−0.82	0.42	−2,657.45	1,142.87
Panel 2						
Main moderation analysis—Rigidity						
Constant	−21.64	11.56	−1.87	0.07	−45.29	2.01
Left thalamus QSM	73.14	158.27	0.46	0.65	−250.58	396.85
Smoking status	−0.27	1.29	−0.21	0.83	−2.91	2.37
Left thalamus QSM × smoking status	−823.74	265.46	−3.10	0.03*	−1,366.68	-280.80
Age	0.14	0.10	0.35	0.19	−0.07	0.35
TIV	0.01	0.01	2.13	0.04	0.00	0.02
Conditional effect of moderator						
Smoking status						
No	496.77	216.95	2.29	0.00*	53.06	940.49
Yes	−326.96	196.18	−1.67	0.11	−728.21	74.28
Panel 3						
Main moderation analysis—H&Y stage						
Constant	3.12	1.04	3.00	0.01*	1.00	5.25
Left SNc QSM	5.67	5.29	1.07	0.29	−5.16	16.49
Smoking status	0.22	0.15	1.46	0.16	−0.09	0.52
Left SNc QSM × smoking status	29.27	10.78	2.71	0.01*	7.21	51.32
Age	0.02	0.01	1.94	0.06	0.00	0.03
TIV	−0.00	0.00	−1.81	0.08	0.00	0.00

Table 4 (*continued*)

Table 4 (*continued*)

Source	B	SE	t	P value	95% CI	
					Lower	Upper
Conditional effect of moderator						
Smoking status						
No	−9.39	5.70	−1.65	0.11	−21.04	2.26
Yes	19.88	8.96	2.22	0.03*	1.56	38.21

The variables were all mean centered for moderation analysis in PROCESS. *, the difference is statistically significant, with a statistical threshold of P<0.05. PD, Parkinson's disease; QSM, quantitative susceptibility mapping; SNc, substantia nigra pars compacta; TIV, total intracranial volume; CI, confidence interval; UPDRS, Unified Parkinson Disease Rating Scale.

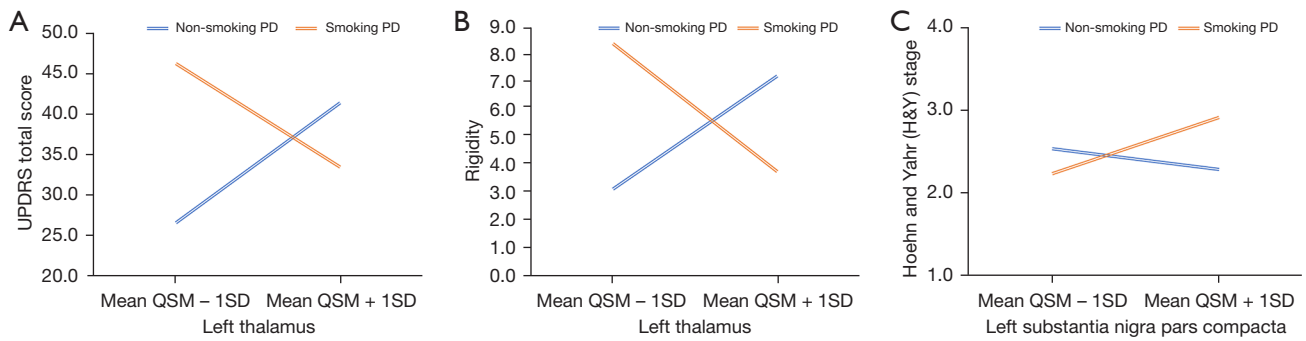

Figure 3 The moderating effect of the interaction of cigarette smoking status (yes/no) and QSM measures in the ROIs on clinical performance in PD patients, with covariates of TIV and age. The slopes changed with the moderator variable of smoking status and exhibited significant interactions illustrated by crossed lines in disordinal forms. (A,B) For non-smokers (blue line) the relationships between the QSM values of the left thalamus and the UPDRS total scores and rigidity severity were positive (the regression line slopes upwards), whereas for smokers (red line), the relationship was negative (the regression line slopes downwards). (C) In non-smokers (blue line), the relationship between the QSM values of the left SNc and the H&Y stages was negative but for smokers (red line) the relationship was positive. QSM, the quantitative susceptibility mapping; ROI, regions of interest; PD, Parkinson's disease; SD, standard deviation; TIV, total intracranial volume; UPDRS, Unified Parkinson Disease Rating Scale; SNc, substantia nigra pars compacta.

−0.43; t=−2.05; P<0.05; right: B=−138.33, 95% CI: −276.47 to −0.19; t=−2.05; P<0.05), rigidity (left: B=−47.52, 95% CI: −83.14 to −11.90; t=−2.73; P=0.01; right: B=−48.12, 95% CI: −87.21 to −9.02; t=−2.52; P=0.02), and bradykinesia scores (left: B=−63.12, 95% CI: −125.65 to −0.58; t=−2.06; P<0.05; right: B=−69.46, 95% CI: −137.16 to −1.75; t=−2.10; P=0.04), and of the right red nucleus and rigidity (B=−10.31, 95% CI: −20.26 to −0.35; t=−2.12; P=0.04) and bradykinesia (B=−19.85, 95% CI: −36.18 to −3.51; t=−2.48; P=0.02) scores (detailed in *Table 5* and *Figure 4*). The disordinal interactions were plotted in the figures by illustrating crossed lines and used to predict clinical performances which were significantly moderated by cigarette smoking status and the SI (*Tables 4,5* and *Figures 3,4*).

The moderation was shown up in PD patients by a significant interaction effect. As illustrated in *Figure 3A,3B*, for PD non-smokers (blue line) the relationships between the QSM values of the left thalamus and the UPDRS total scores and rigidity severity were positive (the regression line slopes upwards), whereas for PD smokers (red line) the relationship was negative (the regression line slopes downwards). However, as for the relationship between the QSM values of the left SNc and H&Y stages (*Figure 3C*), in PD non-smokers (blue line) the relationship was negative but for smokers (red line) the relationship was positive. As illustrated in *Figure 4A-4H*, for heavy-burdened smokers

Table 5 Outputs of moderation analysis for PD patients (moderator variable: smoking index)

Source	B	SE	t	P value	95% CI	
					Lower	Upper
Panel 1						
Main moderation analysis—UPDRS III score						
Constant	−66.44	44.04	−1.51	0.14	−156.52	23.63
Left thalamus QSM	422.66	574.56	0.74	0.47	−752.49	1,597.80
Smoking index	−0.43	0.34	−1.79	0.08	−0.91	0.06
Left thalamus QSM × smoking index	−127.77	62.26	−2.05	<0.05 (0.049)*	−255.11	−0.43
Age	0.99	0.38	2.59	0.01*	0.21	1.78
TIV	0.02	0.02	1.06	0.30	−0.02	0.07
Conditional effect of moderator						
Smoking index						
Mean SI − 1SD	1,217.47	729.39	1.67	0.11	−274.34	2,709.29
Mean SI + 1SD	−1,014.71	852.55	−1.19	0.24	−2,758.42	729.00
Panel 2						
Main moderation analysis—UPDRS III score						
Constant	−52.34	41.92	−1.25	0.22	−138.08	33.39
Right thalamus QSM	497.45	559.96	0.89	0.38	−647.83	1,642.73
Smoking index	−0.20	0.21	−0.95	0.35	−0.63	0.23
Right thalamus QSM × Smoking index	−138.33	67.54	−2.05	<0.05 (0.0497)*	−276.47	−0.19
Age	0.85	0.33	2.59	0.01*	0.18	1.53
TIV	0.02	0.02	0.91	0.37	−0.24	0.06
Conditional effect of moderator						
Smoking index						
Mean SI − 1SD	1,357.94	757.82	1.79	0.08	−192.02	2,907.90
Mean SI + 1SD	−1,058.67	859.38	−1.23	0.23	−2,816.34	699.00
Panel 3						
Main moderation analysis—Rigidity						
Constant	−27.54	12.32	−2.24	0.03	−52.74	−2.34
Left thalamus QSM	107.71	160.73	0.67	0.51	−221.03	436.46
Smoking index	−0.16	0.07	−2.44	0.02*	−0.30	−0.03
Left thalamus QSM × smoking index	−47.52	17.42	−2.73	0.01*	−83.14	−11.90
Age	0.21	0.11	1.94	0.06	−0.01	0.43
TIV	0.01	0.01	2.26	0.03*	0.00	0.26

Table 5 (*continued*)

Table 5 (*continued*)

	B	SE	t	P value	95% CI	
					Lower	Upper
Conditional effect of moderator						
Smoking index						
Mean SI – 1SD	403.32	204.05	1.98	0.06	–14.01	820.65
Mean SI + 1SD	–426.88	238.50	–1.79	0.08	–914.68	60.92
Panel 4						
Main moderation analysis—Rigidity						
Constant	–22.87	11.86	-1.93	0.06	–47.13	1.39
Right thalamus QSM	171.51	158.47	1.08	0.29	–152.60	495.63
Smoking index	–0.08	0.06	–1.35	0.19	–0.20	0.41
Right thalamus QSM × smoking index	–48.12	19.11	–2.52	0.02*	–87.21	–9.02
Age	0.17	0.09	1.85	0.74	–0.02	0.36
TIV	0.01	0.01	2.00	0.05	–0.00	0.02
Conditional effect of moderator						
Smoking index						
Mean SI – 1SD	470.83	214.47	2.20	0.04*	32.18	909.47
Mean SI + 1SD	–369.77	243.21	–1.52	0.14	–867.19	127.66
Panel 5						
Main moderation analysis—Bradykinesia						
Constant	–23.90	21.63	–1.10	0.28	–68.13	20.34
Left thalamus QSM	108.68	282.16	0.39	0.70	–468.41	685.78
Smoking index	–0.19	0.12	–1.59	0.12	–0.43	0.05
Left thalamus QSM × smoking index	–63.12	30.58	–2.06	<0.05 (0.048)*	–125.65	–0.58
Age	0.40	0.19	2.13	0.04*	0.02	0.79
TIV	0.01	0.01	0.74	0.46	-0.01	0.03
Conditional effect of moderator						
Smoking index						
Mean SI – 1SD	501.33	358.19	1.40	0.17	–231.28	1,233.93
Mean SI + 1SD	–601.38	418.68	–1.44	0.16	–1,457.69	254.93
Panel 6						
Main moderation analysis—Bradykinesia						
Constant	–16.76	20.55	–0.82	0.42	–58.78	25.26
Right thalamus QSM	144.49	274.46	0.53	0.60	–416.86	705.85
Smoking index	–0.07	0.10	–0.73	0.47	–0.29	0.14

Table 5 (*continued*)

Table 5 (*continued*)

	B	SE	t	P value	95% CI	
					Lower	Upper
Right thalamus QSM × smoking index	−69.46	33.10	−2.10	0.04*	−137.16	−1.75
Age	0.35	0.16	2.15	0.04*	0.02	0.68
TIV	0.01	0.01	0.52	0.60	−0.02	0.03
Conditional effect of moderator						
Smoking index						
Mean SI − 1SD	576.55	371.44	1.55	0.13	−183.15	1,336.26
Mean SI + 1SD	−636.85	421.22	−1.51	0.14	−1,498.36	224.66
Panel 7						
Main moderation analysis—Rigidity						
Constant	−23.90	12.06	−1.98	0.06	−48.57	0.78
Right red nucleus QSM	20.55	36.81	0.56	0.58	−54.73	95.84
Smoking index	−0.12	0.07	−1.76	0.09	−0.25	0.02
Right red nucleus QSM × smoking index	−10.31	4.87	−2.12	0.04*	−20.26	−0.35
Age	0.14	0.09	1.62	0.12	−0.04	0.32
TIV	0.01	0.01	2.08	0.05	0.00	0.03
Conditional effect of moderator						
Smoking index						
Mean SI − 1SD	84.67	45.94	1.84	0.08	−9.30	178.63
Mean SI + 1SD	-95.39	68.15	−1.40	0.17	−234.78	44.00
Panel 8						
Main moderation analysis—Bradykinesia						
Constant	−26.96	19.79	−1.36	0.18	−67.45	13.52
Right red nucleus QSM	17.94	60.40	0.30	0.77	−105.60	141.48
Smoking index	−0.16	0.11	−1.47	0.15	−0.39	0.06
Right red nucleus QSM × smoking index	−19.85	7.99	−2.48	0.02*	−36.18	−3.51
Age	0.34	0.14	2.38	0.02	0.48	0.63
TIV	0.01	0.01	1.09	0.28	−0.01	0.03
Conditional effect of moderator						
Smoking index						
Mean SI − 1SD	141.39	75.39	1.88	0.07	−12.81	295.59
Mean SI + 1SD	−205.31	111.84	−1.84	0.08	−434.06	23.44

The variables were all mean centered for moderation analysis in PROCESS. *, the difference is statistically significant, with a statistical threshold of $P<0.05$. PD, Parkinson's disease; QSM, quantitative susceptibility mapping; TIV, total intracranial volume; SI, smoking index; SD, standard deviation; CI, confidence interval; UPDRS III, Unified Parkinson Disease Rating Scale III.

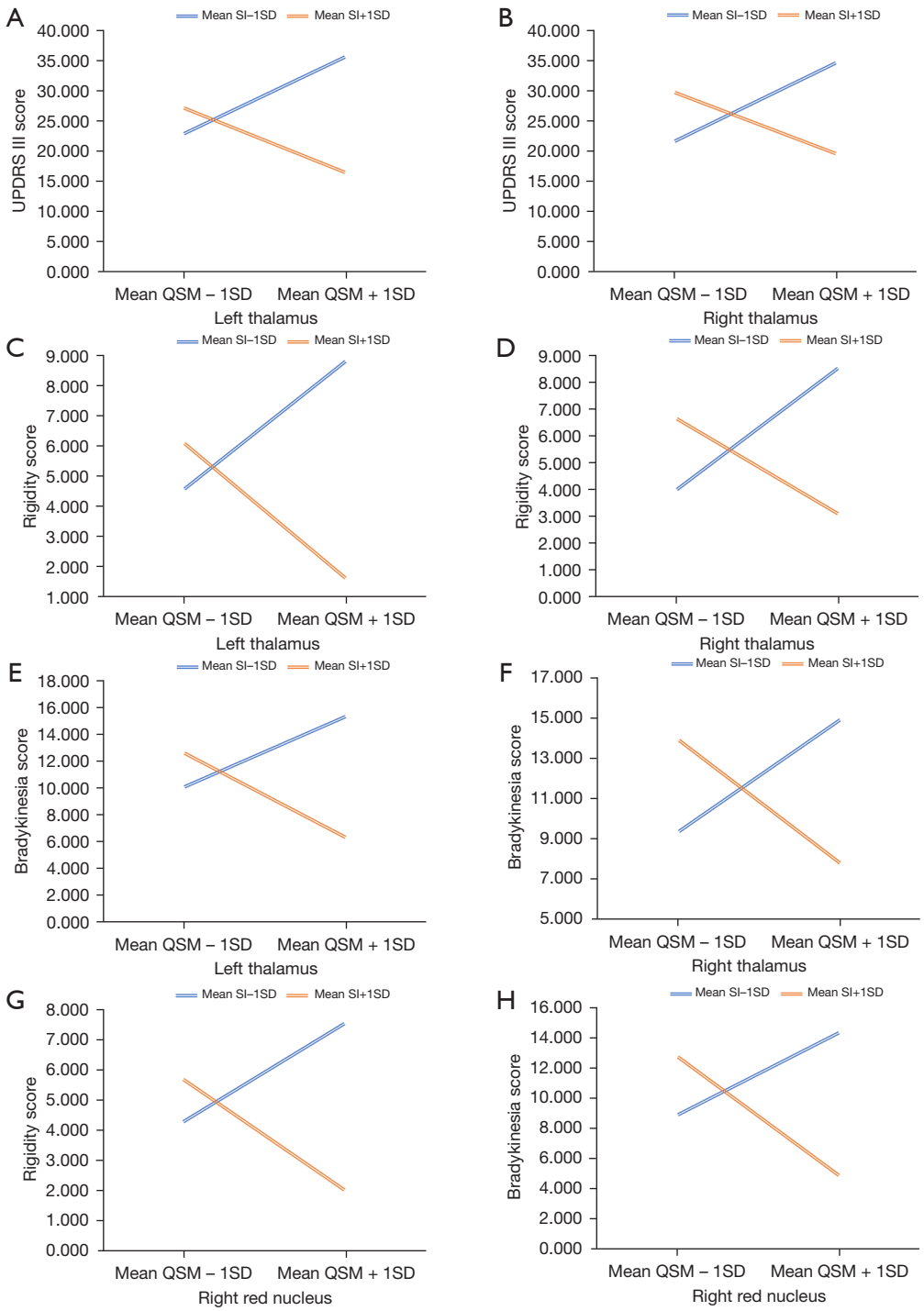

Figure 4 The moderating effect of the interaction of cigarette smoking index and the susceptibility measures in the ROIs on clinical performance in PD patients, with covariates of TIV and age. The slopes changed with the moderator variable of smoking index in disordinal forms. (A-H) For heavy-burdened smokers (mean SI + SD, red line) the relationship between the susceptibility values of bilateral thalami and the UPDRS III score, rigidity and bradykinesia subscores were negative (the regression line slopes downwards), whereas for light-burdened smokers (mean SI − 1SD, blue line) the relationships were positive (the regression line slopes upwards). SI, smoking index; SD, standard deviation; QSM, quantitative susceptibility mapping; ROI, regions of interest; PD, Parkinson's disease; TIV, total intracranial volume; UPDRS III, Unified Parkinson Disease Rating Scale III.

(evidenced by mean SI + 1SD, red line) the relationships between the QSM values of the bilateral thalami and the UPDRS III scores, rigidity, and bradykinesia subscores were negative (the regression line slopes downwards), whereas for light-burdened smokers (evidenced by mean SI – 1SD, blue line) the relationships were positive (the regression line slopes upwards).

Graphically, using smoking status as the moderator variable, when iron deposition of the left thalamus was low (evidenced by the mean QSM – 1SD, as below), PD smokers showed worse performance in general movement disability and rigidity compared with PD non-smokers; conversely, when iron of the left thalamus was high (evidenced by the mean QSM + 1SD, as below), PD smokers showed better general movement disability and rigidity compared with PD non-smokers. In contrast to PD non-smokers, PD smokers stayed at a less severe disease stage when iron deposition of the left SNc was low, but at later stages when iron deposition of the left SNc was high, disease severity increased. Furthermore, using the SI as the moderator variable, we found when iron deposition of the bilateral thalamus was low, heavy-burdened PD smokers (evidenced by mean SI + 1SD, as below) had worse rigidity, bradykinesia, and general movement performance compared to those with a light smoking burden (evidenced by mean SI – 1SD, as below); in contrast, when the iron deposition of the bilateral thalamus was high, heavy-burdened PD smokers showed better aforementioned performance compared with light-burdened PD smokers. Similar outcomes were also present in the right red nucleus, with both rigidity and bradykinesia symptoms.

Discussion

To the best of our knowledge, this was the first study to examine the impacts of different smoking practices (sustained and current smoking versus non-smoking) on PD by means of quantified iron deposition. Since iron overload and resulting neurotoxicity lead to dopamine degradation and alpha-synuclein increase in the nigrostriatal region (35,36), aberrant iron deposition has long been regarded as a marker of PD (37). The QSM technique is best known as a robust, reproducible, and automated technique for imaging tissue susceptibility values from MR phase maps (38,39). Several QSM studies have demonstrated a strong link between brain iron overload and disease severity of PD (2,4,40-42). This technique allows for the qualifiable measurement and distributional depiction of the regional iron concentration for PD patients (2-5).

Numerous studies have confirmed the strong link between cigarette smoking and PD (43-45). Epidemiological evidence has shown that smokers have a lower incidence or severity of PD. The casually protective effect of cigarette smoking on the risk of PD has been repeatedly demonstrated (13,44), with a risk reduction of up to 40% (45). Nicotine is the main ingredient of cigarettes that provides neuroprotection (46,47). It acts as a presynaptic nicotinic acetylcholine receptor (nAChR) agonist that protects against PD (48,49), with a rationale based on the imbalance between nicotinic cholinergic and dopaminergic neurotransmitter systems in the nigrostriatal (19-21). Given previous human and animal studies, the putative biological mechanisms behind nicotine are outlined as follows: (I) activation of nAChRs on dopaminergic terminals to promote dopamine release and improve the efficiency of dopamine transporters in the striatum (50-55); (II) inhibition of the production of free radicals as an antioxidant (56); (III) increase in the levels of both fibroblast growth and neurotrophic factors to stimulate dopaminergic neuron survival (21,57); (IV) elevation of cytochrome P450 enzymes to increase the inactivation of neurotoxins in the brain and delay the development of PD (58); (V) decrease in misfolding and binding of protein to prevent the aggregation of toxic protein α-synuclein (59) and Aβ (60) in the brain; and (VI) mitigation of intestinal inflammation in the gut to change the composition of microbiota and subsequently decrease neuroinflammation in the brain (61). In spite of the reduced incidence of PD that has been repeatedly proposed, no definitive conclusion on smoking has yet been reached since cigarette smoking is still harmful for general health and remains a risk factor for multiple disorders. Thus, caution should be used when interpreting this association as protective, and cigarette smoking is still not recommended.

A major finding in this study was that the smoking-moderated protection for PD symptoms of rigidity, bradykinesia, and general movement performance was consistently present only when the deep brain nuclei were more affected by PD (evidenced by increased iron deposition), regardless of smoking status or smoking index as a moderator variable. In other words, it appeared difficult for cigarette smoking to exacerbate the reduction of physical movement when the PD pathology was mild, whereas cigarette smoking appeared more likely to mitigate symptoms when the PD pathology was serious. Prior to the present study, there had been no other research with similar findings, and we attribute this interesting, double-edged role

of cigarette smoking to the following. First, the smoking-moderated neuroprotection for PD fluctuates, dependent on smoking duration, intensity, and recentness. The neuroprotection is present in a temporal and dose-response manner in PD (62,63). Exposure-disease relationship differs, depending on smoking duration and intensity (62,64), with distinct outcomes (10,65). Acute nicotine administration increases dopamine outputs in the striatum, which initially depresses then increases locomotor activity (66). Chronic nicotine ingestion via transdermal patch, on the other hand, improves motor performance (67) whereas transient cigarette smoking deteriorates it (68). This is due to a high levodopa sensitivity induced by nicotine, which causes a subthreshold stimulation of dopamine release (65) and positive modulators of nAChRs by enhancing striatal dopaminergic function (50). Furthermore, different levels of smoking intensity have distinct impacts on PD. In PD mice models, high doses of nicotine exacerbated 1-methyl-4-phenyl-1,2,3,6-tetrahydropyridine (MPTP)-induced toxicity (69), which was supported by another rat study that found nicotinic neuroprotection was dependent on low, not high, doses by inhibiting neuronal degeneration in the brain (70). Nevertheless, an open trial employing rising doses of transdermal nicotine for the treatment of PD found the opposite results, with the majority of patients tolerating high-dose nicotine and gaining improvement in their clinical symptoms (71). These findings can be explained by a direct action of nicotine, which is mediated by nAChR-pathways (72), or by a D3 receptor upregulation that promotes dopamine use in the central neurological system (73). The nicotinic therapeutic effect is closely connected to the formulations and dosages (68,74-76); the nicotine formulations include patch, gum, administration, nasal spray, and inhaler, and the doses fluctuate widely depending on the tolerance levels of the study participants (70,77). Thus, the reason for these differential results of studies may be related to the variance of smoking/nicotine intake, duration, and intensity among those studies (50). Second, cigarette smoking itself produces distinct effects on different PD motor symptoms. With respect to motor symptoms, some researchers found that the protective effect of smoking worked only on patients dominated by postural instability gait difficulties (PIGD) other than those caused by tremor (78), while other researchers drew the opposite conclusion (74). Likewise, in animal studies, cigarette smoking was found to be effective at managing levodopa-induced bradykinesia (79) and tremor (14). However, cigarette smoking does not benefit all PD motor manifestations. Restless legs syndrome is regarded an early sign of PD, which is aggravated by cigarette smoking (80,81). However, results from other studies using nicotine administration did not find modified motor symptoms (55,82,83), shedding doubts on a direct effect of either nicotine or smoking on PD motor symptoms (49,50). The reason for these differential results is still uncertain, but they may be related to the variance of study paradigms, including smoking habits of participants in those studies (50). Third, other non-motor symptoms are also influenced by smoking-moderated neuroprotection for PD. Those with PD who smoke more often complain of non-motor deficits, such as depression (84), memory difficulties (85), and psychiatric disorders (17,86,87). Severe depression in PD is associated with reduced individual sensation-seeking traits that are involved with mesocorticolimbic dopamine circuits, suggesting that PD, depression, and diminished sensation-seeking traits are likely to share a common neurological substrate (88). This assumption is supported by the decreased novelty seeking found in PD patients, making patients less prone to consume stimulants like cigarettes (89) and to subsequently change their smoking practices, such as duration and intensity. Memory problems usually predict the cognitive impairment of PD (90). The causal interaction between smoking and cognitive dysfunction is still unclear, but excessive iron deposition in deep brain nuclei could cause neurotoxicity, neuroinflammation, and the aggregation of Lewy bodies and abnormal build-up of alpha (α)-synuclein, leading to cognitive deficits in PD (91-94). Impulse-control disorder (ICD) is one of the most common psychiatric disorders in PD smokers, whereby smoking (19) and mutated genes (95) jointly participate in the upregulation of sensitivity in developing and maintaining behavioral symptoms. In addition, motor and non-motor symptoms co-interact in the context of smoking. For example, smoking exposure-associated negative mood may potentially worsen the motor symptoms of PD patients with a smoking history than those without (10). Tremor-dominated PD patients are more likely to be current smokers but present with fewer non-motor symptoms (78). Moreover, the transient deterioration of specific motor and non-motor symptoms has been observed in some PD patients with a smoking history (10,65). Taken together, we assumed that an unknown trigger point might exist for this exposure-disease relationship. In other words, once the pathological changes of PD reach a certain level, smoking may exert its effects in moderating neuroprotection against PD symptoms.

Another significant finding in this study by moderation analyses is that the thalamus, red nucleus, and SN were the nuclei most moderated by cigarette smoking, as evidenced by the brain iron-PD interaction. As a proxy for iron deposition, previous QSM studies have continuously demonstrated that changes in QSM values externalize excessive iron load in the nuclei, reflecting pathological changes in the PD brain (5,96-99). Notably, in this study, both smoking status and burdens moderated the interaction between the thalamic pathology and movement slowness (i.e., rigidity and bradykinesia) in PD smokers. Anatomically, the thalamus is located between the midbrain and cortices to relay and filter information for further processing (100), exhibiting different roles in PD clinical symptoms. Pathophysiologically, the thalamus plays a dual role in both cholinergic and dopaminergic systems, having the highest density of nAChRs in the brain and simultaneously serving as a central hub for the formation of the classical cortico-striato-nigro-thalamo-cortical and cerebello-thalamo-cortical pathways of PD (101-103). Many studies have found changes in the morphology and function of the thalamus in smokers relative to non-smokers (103,104), which are mainly attributed to the nicotine-induced regulation of nAChRs (105) and the dysfunction of the cortico-basal ganglia-thalamo-cortical reward circuit as well (106). The thalamus, as the region with the most accumulation of AChR, receives plenty of cholinergic inputs from the brainstem center (107). Thalamic cholinergic denervation has been repeatedly found in PD patients compared with controls (108,109), which is supported by the fact that anticholinergic drugs have been commonly used to suppress excessive movements, such as tremor symptom (10). As previously shown in a single-photon emission computerized tomography (SPECT) study, after smoking cessation, the upregulated nAChR levels of the smokers returned to normal (110), which suggested that the smoking-moderated upregulation may be temporary and delayed during the course of smoking. Consequently, the following neuroprotection is unlikely to be fixed. On this basis, the presence of thalamic neuroprotection for decreased movements of rigidity and bradykinesia rather than tremor is likely to indicate activation of the cholinergic system in the thalamus of PD patients. In addition to acetylcholine, certain components in cigarettes can irreversibly inhibit the activity of monoamine oxidases (MAOs) in the basal ganglia (111). For this reason, rasagiline is an MAO inhibitor currently used for the treatment of PD (112). Taken together, the thalamus does exert essential impacts on cigarette smoking and PD, but the causal relationships is unclear, and the outcomes are still variable. This suggests that smoking-moderated neuroprotection is the result of a joint effort involving multiple neurotransmitter systems.

Except for the thalamus, the red nucleus has been identified as one of the most significant iron deposition regions affected by PD (36,113). When using the SI as a moderator variable, the slope directions for rigidity and bradykinesia in the red nucleus were consistent with those of the bilateral thalami, suggesting a potential causal relationship between the red nucleus and the thalamus. The dentato-rubro-thalamic tract has been widely used as a deep brain stimulation target for tremor-specific suppression in PD (114), but in our moderation analysis the impaired red nucleus was found more closely correlated to rigidity and bradykinesia than tremor in PD patients. Similar to the findings in the thalamus, we considered that this was possibly due to receptor desensitization, suggesting the threshold of smoking burden indeed deserves special attention for studying the neuroprotection of cigarette smoking.

In addition, our present study showed the relationship between the iron deposition of the left SNc and the H&Y stages for PD smokers was positive; that is, cigarette smoking could not reverse progressive degradation in the left SNc. Based on our previous study, iron deposition in the SNc was found to be affected exclusively in the early stages of PD (4), which has been supported by other similar findings (115,116). The underlying mechanism is still unclear, but the potential reason is likely attributable to decreased neuromelanin in the SNc of PD, which has been shown to play an essential and exclusive role in PD (117-119). Moreover, the redistributed iron in the brain according to metabolism in the early stages of PD may be also involved (120). Supported by findings of previous animal studies, this disordinal moderating effect observed in our study suggested that nicotine-induced neuroprotection for PD was likely to act only on progressive striatal degenerative alterations, delaying and stopping the unhappened progression of PD, but not on reversing the damage to the dopaminergic system that has already occurred (20,121). Our findings suggest that cigarette smoking starts to take a protective effect by disrupting the iron redistribution process at an early stage of PD, which requires verification in future research.

This study had some limitations. First, we did not enroll past smokers into the study. The effect of previous smoking history on PD has remained unclear among different

clinical studies (10,63) and, as yet, we have not found a direct link between the iron deposition in PD and that of ex-smokers; however, a temporal relationship between smoking history and PD and the potential mechanism for abnormal iron load has been highly suggested. Ex-smokers have a markedly decreased risk of developing PD compared with never smokers (43). Furthermore, the lower risk of PD among current and ex-smokers varies with smoking duration, intensity, and recentness (62). Further research needs to be conducted on the impact of different types of smoking habits on PD. Second, we used iron deposition of the major deep brain nuclei as a proxy for PD pathology, but this did not turn into iron deposition in cortical or white matter structures. The relationship between iron metabolism and changes in morphology is still uncertain, and more modals of data need to be collected in future. Third, the effect of cigarette smoking on PD varies with the smoking condition, as discussed in the paper, and longitudinal follow-up studies are necessary to better elucidate the role of cigarette smoking in PD.

Conclusions

To the best of our knowledge, this was the first study to investigate the impacts of current cigarette smoking on PD using quantified iron deposition as a surrogate biomarker for PD pathology. We concluded our major findings as follows: (I) cigarette smoking moderates the interaction between the iron content of the deep brain nuclei and rigidity, bradykinesia, and general performance of PD patients in a double-edged fashion; and (II) in the interaction between iron deposition and clinical PD symptoms, the thalamus, red nucleus, and SNc are the nuclei most affected by cigarette smoking. These findings may help understand the protective role of cigarette smoking against PD.

Acknowledgments

Funding: This work was supported by the National Natural Science Foundation of China (No. 81701647).

Footnote

Reporting Checklist: The authors have completed the STROBE reporting checklist. Available at https://qims.amegroups.com/article/view/10.21037/qims-21-1090/rc

Conflicts of Interest: All authors have completed the ICMJE uniform disclosure form (available at https://qims.amegroups.com/article/view/10.21037/qims-21-1090/coif). QG reports that this work was supported by the National Natural Science Foundation of China (No. 81701647). The other authors have no conflicts of interest to declare.

Ethical Statement: The authors are accountable for all aspects of the work in ensuring that questions related to the accuracy or integrity of any part of the work are appropriately investigated and resolved. The study was conducted in accordance with the Declaration of Helsinki (as revised in 2013). The study was approved by the Ethical Review Board at Zhejiang University and informed consent was provided by all participants.

References

1. Dickson DW. Neuropathology of Parkinson disease. Parkinsonism Relat Disord 2018;46 Suppl 1:S30-3.
2. Guan X, Guo T, Zhou C, Wu J, Gao T, Bai X, Wei H, Zhang Y, Xuan M, Gu Q, Huang P, Liu C, Zhang B, Pu J, Song Z, Yan Y, Cui F, Zhang M, Xu X. Asymmetrical nigral iron accumulation in Parkinson's disease with motor asymmetry: an explorative, longitudinal and test-retest study. Aging (Albany NY) 2020. [Epub ahead of print].
3. Guan X, Xu X, Zhang M. Region-Specific Iron Measured by MRI as a Biomarker for Parkinson's Disease. Neurosci Bull 2017;33:561-7.
4. Guan X, Xuan M, Gu Q, Huang P, Liu C, Wang N, Xu X, Luo W, Zhang M. Regionally progressive accumulation of iron in Parkinson's disease as measured by quantitative susceptibility mapping. NMR Biomed 2017.
5. Guan X, Zhang Y, Wei H, Guo T, Zeng Q, Zhou C, Wang J, Gao T, Xuan M, Gu Q, Xu X, Huang P, Pu J, Zhang B, Liu C, Zhang M. Iron-related nigral degeneration influences functional topology mediated by striatal dysfunction in Parkinson's disease. Neurobiol Aging 2019;75:83-97.

6. Ambrose JA, Barua RS. The pathophysiology of cigarette smoking and cardiovascular disease: an update. J Am Coll Cardiol 2004;43:1731-7.
7. Jenner P. Oxidative stress in Parkinson's disease. Ann Neurol 2003;53 Suppl 3:S26-36; discussion S36-8.
8. Ascherio A, Schwarzschild MA. The epidemiology of Parkinson's disease: risk factors and prevention. Lancet Neurol 2016;15:1257-72.
9. Lee PC, Ahmed I, Loriot MA, Mulot C, Paul KC, Bronstein JM, Ritz B, Elbaz A. Smoking and Parkinson disease: Evidence for gene-by-smoking interactions. Neurology 2018;90:e583-92.
10. Neshige S, Ohshita T, Neshige R, Maruyama H. Influence of current and previous smoking on current phenotype in Parkinson's disease. J Neurol Sci 2021;427:117534.
11. Lee Y, Oh JS, Chung SJ, Chung SJ, Kim SJ, Nam CM, Lee PH, Kim JS, Sohn YH. Does smoking impact dopamine neuronal loss in de novo Parkinson disease? Ann Neurol 2017;82:850-4.
12. Kandinov B, Giladi N, Korczyn AD. Smoking and tea consumption delay onset of Parkinson's disease. Parkinsonism Relat Disord 2009;15:41-6.
13. Li X, Li W, Liu G, Shen X, Tang Y. Association between cigarette smoking and Parkinson's disease: A meta-analysis. Arch Gerontol Geriatr 2015;61:510-6.
14. Marshall J, Schnieden H. Effect of adrenaline, noradrenaline, atropine, and nicotine on some types of human tremor. J Neurol Neurosurg Psychiatry 1966;29:214-8.
15. Quik M, Cox H, Parameswaran N, O'Leary K, Langston JW, Di Monte D. Nicotine reduces levodopa-induced dyskinesias in lesioned monkeys. Ann Neurol 2007;62:588-96.
16. Moccia M, Mollenhauer B, Erro R, Picillo M, Palladino R, Barone P. Non-Motor Correlates of Smoking Habits in de Novo Parkinson's Disease. J Parkinsons Dis 2015;5:913-24.
17. Morgante F, Fasano A, Ginevrino M, Petrucci S, Ricciardi L, Bove F, Criscuolo C, Moccia M, De Rosa A, Sorbera C, Bentivoglio AR, Barone P, De Michele G, Pellecchia MT, Valente EM. Impulsive-compulsive behaviors in parkin-associated Parkinson disease. Neurology 2016;87:1436-41.
18. Zhang JF, Wang XX, Feng Y, Fekete R, Jankovic J, Wu YC. Impulse Control Disorders in Parkinson's Disease: Epidemiology, Pathogenesis and Therapeutic Strategies. Front Psychiatry 2021;12:635494.
19. Zhou FM, Wilson CJ, Dani JA. Cholinergic interneuron characteristics and nicotinic properties in the striatum. J Neurobiol 2002;53:590-605.
20. Perez XA. Preclinical Evidence for a Role of the Nicotinic Cholinergic System in Parkinson's Disease. Neuropsychol Rev 2015;25:371-83.
21. Maggio R, Riva M, Vaglini F, Fornai F, Molteni R, Armogida M, Racagni G, Corsini GU. Nicotine prevents experimental parkinsonism in rodents and induces striatal increase of neurotrophic factors. J Neurochem 1998;71:2439-46.
22. Reichmann H. Clinical criteria for the diagnosis of Parkinson's disease. Neurodegener Dis 2010;7:284-90.
23. Hoehn MM, Yahr MD. Parkinsonism: onset, progression, and mortality. 1967. Neurology 2001;57:S11-26.
24. Goetz CG, Fahn S, Martinez-Martin P, Poewe W, Sampaio C, Stebbins GT, et al. Movement Disorder Society-sponsored revision of the Unified Parkinson's Disease Rating Scale (MDS-UPDRS): Process, format, and clinimetric testing plan. Mov Disord 2007;22:41-7.
25. Folstein MF, Folstein SE, McHugh PR. "Mini-mental state". A practical method for grading the cognitive state of patients for the clinician. J Psychiatr Res 1975;12:189-98.
26. Indrayan A, Kumar R, Dwivedi S. A simple index of smoking. COBRA Preprint Series (Berkeley Electronic Press), Article 41, (2008).
27. Hu T. Tobacco Control Policy Analysis in China: Economics and Health. World Scientific Publishing Company, 2008.
28. Volkov VV, Zhu Y. Deterministic phase unwrapping in the presence of noise. Opt Lett 2003;28:2156-8.
29. Wu B, Li W, Guidon A, Liu C. Whole brain susceptibility mapping using compressed sensing. Magn Reson Med 2012;67:137-47.
30. Li W, Wu B, Liu C. Quantitative susceptibility mapping of human brain reflects spatial variation in tissue composition. Neuroimage 2011;55:1645-56.
31. Wei H, Dibb R, Zhou Y, Sun Y, Xu J, Wang N, Liu C. Streaking artifact reduction for quantitative susceptibility mapping of sources with large dynamic range. NMR Biomed 2015;28:1294-303.
32. Wei H, Zhang Y, Gibbs E, Chen NK, Wang N, Liu C. Joint 2D and 3D phase processing for quantitative susceptibility mapping: application to 2D echo-planar imaging. NMR Biomed 2017.
33. Zhang Y, Wei H, Cronin MJ, He N, Yan F, Liu C. Longitudinal atlas for normative human brain development and aging over the lifespan using quantitative susceptibility mapping. Neuroimage 2018;171:176-89.
34. Hayes AF, Preacher KJ. Conditional process modeling:

Using structural equation modeling to examine contingent causal processes. In: Hancock GR, Mueller RO. editors. Structural equation modeling: A second course. IAP Information Age Publishing, 2013:219-66.
35. Wan W, Jin L, Wang Z, Wang L, Fei G, Ye F, Pan X, Wang C, Zhong C. Iron Deposition Leads to Neuronal α-Synuclein Pathology by Inducing Autophagy Dysfunction. Front Neurol 2017;8:1.
36. Shahmaei V, Faeghi F, Mohammdbeigi A, Hashemi H, Ashrafi F. Evaluation of iron deposition in brain basal ganglia of patients with Parkinson's disease using quantitative susceptibility mapping. Eur J Radiol Open 2019;6:169-74.
37. Acosta-Cabronero J, Cardenas-Blanco A, Betts MJ, Butryn M, Valdes-Herrera JP, Galazky I, Nestor PJ. The whole-brain pattern of magnetic susceptibility perturbations in Parkinson's disease. Brain 2017;140:118-31.
38. Li L, Leigh JS. Quantifying arbitrary magnetic susceptibility distributions with MR. Magn Reson Med 2004;51:1077-82.
39. Zhang X, Guo Y, Chen Y, Mei Y, Chen J, Wang J, Feng Y, Zhang X. Reproducibility of quantitative susceptibility mapping in lumbar vertebra. Quant Imaging Med Surg 2019;9:691-9.
40. Thomas GEC, Leyland LA, Schrag AE, Lees AJ, Acosta-Cabronero J, Weil RS. Brain iron deposition is linked with cognitive severity in Parkinson's disease. J Neurol Neurosurg Psychiatry 2020;91:418-25.
41. Uchida Y, Kan H, Sakurai K, Arai N, Kato D, Kawashima S, Ueki Y, Matsukawa N. Voxel-based quantitative susceptibility mapping in Parkinson's disease with mild cognitive impairment. Mov Disord 2019;34:1164-73.
42. Uchida Y, Kan H, Sakurai K, Inui S, Kobayashi S, Akagawa Y, Shibuya K, Ueki Y, Matsukawa N. Magnetic Susceptibility Associates With Dopaminergic Deficits and Cognition in Parkinson's Disease. Mov Disord 2020;35:1396-405.
43. Gallo V, Vineis P, Cancellieri M, Chiodini P, Barker RA, Brayne C, et al. Exploring causality of the association between smoking and Parkinson's disease. Int J Epidemiol 2019;48:912-25.
44. Mappin-Kasirer B, Pan H, Lewington S, Kizza J, Gray R, Clarke R, Peto R. Tobacco smoking and the risk of Parkinson disease: A 65-year follow-up of 30,000 male British doctors. Neurology 2020;94:e2132-8.
45. Hernán MA, Takkouche B, Caamaño-Isorna F, Gestal-Otero JJ. A meta-analysis of coffee drinking, cigarette smoking, and the risk of Parkinson's disease. Ann Neurol 2002;52:276-84.
46. Barreto GE, Iarkov A, Moran VE. Beneficial effects of nicotine, cotinine and its metabolites as potential agents for Parkinson's disease. Front Aging Neurosci 2015;6:340.
47. Ross GW, Petrovitch H. Current evidence for neuroprotective effects of nicotine and caffeine against Parkinson's disease. Drugs Aging 2001;18:797-806.
48. Quik M, Bordia T, Huang L, Perez X. Targeting nicotinic receptors for Parkinson's disease therapy. CNS Neurol Disord Drug Targets 2011;10:651-8.
49. Quik M, O'Leary K, Tanner CM. Nicotine and Parkinson's disease: implications for therapy. Mov Disord 2008;23:1641-52.
50. Quik M, Perez XA, Bordia T. Nicotine as a potential neuroprotective agent for Parkinson's disease. Mov Disord 2012;27:947-57.
51. Tsuang D, Larson EB, Li G, Shofer JB, Montine KS, Thompson ML, Sonnen JA, Crane PK, Leverenz JB, Montine TJ. Association between lifetime cigarette smoking and lewy body accumulation. Brain Pathol 2010;20:412-8.
52. Gigante AF, Defazio G, Niccoli Asabella A, Superbo M, Ferrari C, Liuzzi D, Iliceto G, Livrea P, Rubini G. Smoking in Patients with Parkinson's Disease: preliminary striatal DaT-SPECT findings. Acta Neurol Scand 2016;134:265-70.
53. Grady SR, Salminen O, Laverty DC, Whiteaker P, McIntosh JM, Collins AC, Marks MJ. The subtypes of nicotinic acetylcholine receptors on dopaminergic terminals of mouse striatum. Biochem Pharmacol 2007;74:1235-46.
54. Quik M, Wonnacott S. α6β2* and α4β2* nicotinic acetylcholine receptors as drug targets for Parkinson's disease. Pharmacol Rev 2011;63:938-66.
55. Huang LZ, Grady SR, Quik M. Nicotine reduces L-DOPA-induced dyskinesias by acting at beta2* nicotinic receptors. J Pharmacol Exp Ther 2011;338:932-41.
56. Fowler JS, Volkow ND, Wang GJ, Pappas N, Logan J, MacGregor R, Alexoff D, Shea C, Schlyer D, Wolf AP, Warner D, Zezulkova I, Cilento R. Inhibition of monoamine oxidase B in the brains of smokers. Nature 1996;379:733-6.
57. Bean AJ, Elde R, Cao YH, Oellig C, Tamminga C, Goldstein M, Pettersson RF, Hökfelt T. Expression of acidic and basic fibroblast growth factors in the substantia nigra of rat, monkey, and human. Proc Natl Acad Sci U S A 1991;88:10237-41.
58. Miksys S, Tyndale RF. Nicotine induces brain CYP

enzymes: relevance to Parkinson's disease. J Neural Transm Suppl 2006;(70):177-80.
59. Hong DP, Fink AL, Uversky VN. Smoking and Parkinson's disease: does nicotine affect alpha-synuclein fibrillation? Biochim Biophys Acta 2009;1794:282-90.
60. Jin L, Wang J, Zhao L, Jin H, Fei G, Zhang Y, Zeng M, Zhong C. Decreased serum ceruloplasmin levels characteristically aggravate nigral iron deposition in Parkinson's disease. Brain 2011;134:50-8.
61. Derkinderen P, Shannon KM, Brundin P. Gut feelings about smoking and coffee in Parkinson's disease. Mov Disord 2014;29:976-9.
62. Thacker EL, O'Reilly EJ, Weisskopf MG, Chen H, Schwarzschild MA, McCullough ML, Calle EE, Thun MJ, Ascherio A. Temporal relationship between cigarette smoking and risk of Parkinson disease. Neurology 2007;68:764-8.
63. Chen H, Huang X, Guo X, Mailman RB, Park Y, Kamel F, Umbach DM, Xu Q, Hollenbeck A, Schatzkin A, Blair A. Smoking duration, intensity, and risk of Parkinson disease. Neurology 2010;74:878-84.
64. Gorell JM, Rybicki BA, Johnson CC, Peterson EL. Smoking and Parkinson's disease: a dose-response relationship. Neurology 1999;52:115-9.
65. Ling H, Petrovic I, Day BL, Lees AJ. Smoking-induced transient motor deterioration in a levodopa-treated patient with Parkinson's disease. J Neurol 2012;259:2419-23.
66. Seppä T, Ahtee L. Comparison of the effects of epibatidine and nicotine on the output of dopamine in the dorsal and ventral striatum of freely-moving rats. Naunyn Schmiedebergs Arch Pharmacol 2000;362:444-7.
67. Kelton MC, Kahn HJ, Conrath CL, Newhouse PA. The effects of nicotine on Parkinson's disease. Brain Cogn 2000;43:274-82.
68. Ebersbach G, Stöck M, Müller J, Wenning G, Wissel J, Poewe W. Worsening of motor performance in patients with Parkinson's disease following transdermal nicotine administration. Mov Disord 1999;14:1011-3.
69. Behmand RA, Harik SI. Nicotine enhances 1-methyl-4-phenyl-1,2,3,6-tetrahydropyridine neurotoxicity. J Neurochem 1992;58:776-9.
70. Ryan RE, Ross SA, Drago J, Loiacono RE. Dose-related neuroprotective effects of chronic nicotine in 6-hydroxydopamine treated rats, and loss of neuroprotection in alpha4 nicotinic receptor subunit knockout mice. Br J Pharmacol 2001;132:1650-6.
71. Villafane G, Cesaro P, Rialland A, Baloul S, Azimi S, Bourdet C, Le Houezec J, Macquin-Mavier I, Maison P. Chronic high dose transdermal nicotine in Parkinson's disease: an open trial. Eur J Neurol 2007;14:1313-6.
72. Wonnacott S, Kaiser S, Mogg A, Soliakov L, Jones IW. Presynaptic nicotinic receptors modulating dopamine release in the rat striatum. Eur J Pharmacol 2000;393:51-8.
73. Le Foll B, Diaz J, Sokoloff P. Increased dopamine D3 receptor expression accompanying behavioral sensitization to nicotine in rats. Synapse 2003;47:176-83.
74. Ishikawa A, Miyatake T. Effects of smoking in patients with early-onset Parkinson's disease. J Neurol Sci 1993;117:28-32.
75. Clemens P, Baron JA, Coffey D, Reeves A. The short-term effect of nicotine chewing gum in patients with Parkinson's disease. Psychopharmacology (Berl) 1995;117:253-6.
76. Nishimura H, Tachibana H, Okuda B, Sugita M. Transient worsening of Parkinson's disease after cigarette smoking. Intern Med 1997;36:651-3.
77. Villafane G, Thiriez C, Audureau E, Straczek C, Kerschen P, Cormier-Dequaire F, Van Der Gucht A, Gurruchaga JM, Quéré-Carne M, Evangelista E, Paul M, Defer G, Damier P, Remy P, Itti E, Fénelon G. High-dose transdermal nicotine in Parkinson's disease patients: a randomized, open-label, blinded-endpoint evaluation phase 2 study. Eur J Neurol 2018;25:120-7.
78. Skeie GO, Muller B, Haugarvoll K, Larsen JP, Tysnes OB. Differential effect of environmental risk factors on postural instability gait difficulties and tremor dominant Parkinson's disease. Mov Disord 2010;25:1847-52.
79. Zhang D, Bordia T, McGregor M, McIntosh JM, Decker MW, Quik M. ABT-089 and ABT-894 reduce levodopa-induced dyskinesias in a monkey model of Parkinson's disease. Mov Disord 2014;29:508-17.
80. Lavigne GL, Lobbezoo F, Rompré PH, Nielsen TA, Montplaisir J. Cigarette smoking as a risk factor or an exacerbating factor for restless legs syndrome and sleep bruxism. Sleep 1997;20:290-3.
81. Phillips B, Young T, Finn L, Asher K, Hening WA, Purvis C. Epidemiology of restless legs symptoms in adults. Arch Intern Med 2000;160:2137-41.
82. Quik M, Mallela A, Ly J, Zhang D. Nicotine reduces established levodopa-induced dyskinesias in a monkey model of Parkinson's disease. Mov Disord 2013;28:1398-406.
83. Bordia T, Campos C, Huang L, Quik M. Continuous and intermittent nicotine treatment reduces L-3,4-dihydroxyphenylalanine (L-DOPA)-induced dyskinesias in a rat model of Parkinson's disease. J Pharmacol Exp Ther 2008;327:239-47.

84. Gigante AF, Martino T, Iliceto G, Defazio G. Smoking and age-at-onset of both motor and non-motor symptoms in Parkinson's disease. Parkinsonism Relat Disord 2017;45:94-6.
85. Weisskopf MG, Grodstein F, Ascherio A. Smoking and cognitive function in Parkinson's disease. Mov Disord 2007;22:660-5.
86. Weintraub D, Koester J, Potenza MN, Siderowf AD, Stacy M, Voon V, Whetteckey J, Wunderlich GR, Lang AE. Impulse control disorders in Parkinson disease: a cross-sectional study of 3090 patients. Arch Neurol 2010;67:589-95.
87. Bastiaens J, Dorfman BJ, Christos PJ, Nirenberg MJ. Prospective cohort study of impulse control disorders in Parkinson's disease. Mov Disord 2013;28:327-33.
88. Taylor AE, Fluharty ME, Bjørngaard JH, Gabrielsen ME, Skorpen F, Marioni RE, et al. Investigating the possible causal association of smoking with depression and anxiety using Mendelian randomisation meta-analysis: the CARTA consortium. BMJ Open 2014;4:e006141.
89. Evans AH, Lawrence AD, Potts J, MacGregor L, Katzenschlager R, Shaw K, Zijlmans J, Lees AJ. Relationship between impulsive sensation seeking traits, smoking, alcohol and caffeine intake, and Parkinson's disease. J Neurol Neurosurg Psychiatry 2006;77:317-21.
90. Ritz B, Lee PC, Lassen CF, Arah OA. Parkinson disease and smoking revisited: ease of quitting is an early sign of the disease. Neurology 2014;83:1396-402.
91. Erro R, Santangelo G, Barone P, Picillo M, Amboni M, Longo K, Giordano F, Moccia M, Allocca R, Pellecchia MT, Vitale C. Do subjective memory complaints herald the onset of mild cognitive impairment in Parkinson disease? J Geriatr Psychiatry Neurol 2014;27:276-81.
92. Saari L, Kivinen K, Gardberg M, Joutsa J, Noponen T, Kaasinen V. Dopamine transporter imaging does not predict the number of nigral neurons in Parkinson disease. Neurology 2017;88:1461-7.
93. Apostolova LG, Beyer M, Green AE, Hwang KS, Morra JH, Chou YY, Avedissian C, Aarsland D, Janvin CC, Larsen JP, Cummings JL, Thompson PM. Hippocampal, caudate, and ventricular changes in Parkinson's disease with and without dementia. Mov Disord 2010;25:687-95.
94. Oh YS, Kim JS, Hwang EJ, Lyoo CH. Striatal dopamine uptake and olfactory dysfunction in patients with early Parkinson's disease. Parkinsonism Relat Disord 2018;56:47-51.
95. Brody AL, Mandelkern MA, Olmstead RE, Scheibal D, Hahn E, Shiraga S, Zamora-Paja E, Farahi J, Saxena S, London ED, McCracken JT. Gene variants of brain dopamine pathways and smoking-induced dopamine release in the ventral caudate/nucleus accumbens. Arch Gen Psychiatry 2006;63:808-16.
96. Chen J, Cai T, Li Y, Chi J, Rong S, He C, Li X, Zhang P, Wang L, Zhang Y. Different iron deposition patterns in Parkinson's disease subtypes: a quantitative susceptibility mapping study. Quant Imaging Med Surg 2020;10:2168-76.
97. He N, Ling H, Ding B, Huang J, Zhang Y, Zhang Z, Liu C, Chen K, Yan F. Region-specific disturbed iron distribution in early idiopathic Parkinson's disease measured by quantitative susceptibility mapping. Hum Brain Mapp 2015;36:4407-20.
98. Chen Q, Chen Y, Zhang Y, Wang F, Yu H, Zhang C, Jiang Z, Luo W. Iron deposition in Parkinson's disease by quantitative susceptibility mapping. BMC Neurosci 2019;20:23.
99. Barbosa JH, Santos AC, Tumas V, Liu M, Zheng W, Haacke EM, Salmon CE. Quantifying brain iron deposition in patients with Parkinson's disease using quantitative susceptibility mapping, R2 and R2. Magn Reson Imaging 2015;33:559-65.
100. Moustafa AA, McMullan RD, Rostron B, Hewedi DH, Haladjian HH. The thalamus as a relay station and gatekeeper: relevance to brain disorders. Rev Neurosci 2017;28:203-18.
101. Gu Q, Cao H, Xuan M, Luo W, Guan X, Xu J, Huang P, Zhang M, Xu X. Increased thalamic centrality and putamen-thalamic connectivity in patients with parkinsonian resting tremor. Brain Behav 2016;7:e00601.
102. McGregor MM, Nelson AB. Circuit Mechanisms of Parkinson's Disease. Neuron 2019;101:1042-56.
103. Wang C, Wang S, Shen Z, Qian W, Jiaerken Y, Luo X, Li K, Zeng Q, Gu Q, Yang Y, Huang P, Zhang M. Increased thalamic volume and decreased thalamo-precuneus functional connectivity are associated with smoking relapse. Neuroimage Clin 2020;28:102451.
104. Sutherland MT, Riedel MC, Flannery JS, Yanes JA, Fox PT, Stein EA, Laird AR. Chronic cigarette smoking is linked with structural alterations in brain regions showing acute nicotinic drug-induced functional modulations. Behav Brain Funct 2016;12:16.
105. Staley JK, Krishnan-Sarin S, Cosgrove KP, Krantzler E, Frohlich E, Perry E, Dubin JA, Estok K, Brenner E, Baldwin RM, Tamagnan GD, Seibyl JP, Jatlow P, Picciotto MR, London ED, O'Malley S, van Dyck CH. Human tobacco smokers in early abstinence have higher levels of beta2* nicotinic acetylcholine receptors than nonsmokers.

J Neurosci 2006;26:8707-14.
106. Huang AS, Mitchell JA, Haber SN, Alia-Klein N, Goldstein RZ. The thalamus in drug addiction: from rodents to humans. Philos Trans R Soc Lond B Biol Sci 2018;373:20170028.
107. Bohnen NI, Albin RL. The cholinergic system and Parkinson disease. Behav Brain Res 2011;221:564-73.
108. Shinotoh H, Namba H, Yamaguchi M, Fukushi K, Nagatsuka S, Iyo M, Asahina M, Hattori T, Tanada S, Irie T. Positron emission tomographic measurement of acetylcholinesterase activity reveals differential loss of ascending cholinergic systems in Parkinson's disease and progressive supranuclear palsy. Ann Neurol 1999;46:62-9.
109. Müller ML, Albin RL, Kotagal V, Koeppe RA, Scott PJ, Frey KA, Bohnen NI. Thalamic cholinergic innervation and postural sensory integration function in Parkinson's disease. Brain 2013;136:3282-9.
110. Mamede M, Ishizu K, Ueda M, Mukai T, Iida Y, Kawashima H, Fukuyama H, Togashi K, Saji H. Temporal change in human nicotinic acetylcholine receptor after smoking cessation: 5IA SPECT study. J Nucl Med 2007;48:1829-35.
111. Sharma A, Brody AL. In vivo brain imaging of human exposure to nicotine and tobacco. Handb Exp Pharmacol 2009;(192):145-71.
112. Weinreb O, Amit T, Bar-Am O, Youdim MB. Rasagiline: a novel anti-Parkinsonian monoamine oxidase-B inhibitor with neuroprotective activity. Prog Neurobiol 2010;92:330-44.
113. Du G, Lewis MM, Sen S, Wang J, Shaffer ML, Styner M, Yang QX, Huang X. Imaging nigral pathology and clinical progression in Parkinson's disease. Mov Disord 2012;27:1636-43.
114. Coenen VA, Sajonz B, Prokop T, Reisert M, Piroth T, Urbach H, Jenkner C, Reinacher PC. The dentato-rubro-thalamic tract as the potential common deep brain stimulation target for tremor of various origin: an observational case series. Acta Neurochir (Wien) 2020;162:1053-66.
115. Martin WR, Wieler M, Gee M. Midbrain iron content in early Parkinson disease: a potential biomarker of disease status. Neurology 2008;70:1411-7.
116. Wang C, Fan G, Xu K, Wang S. Quantitative assessment of iron deposition in the midbrain using 3D-enhanced T2 star weighted angiography (ESWAN): a preliminary cross-sectional study of 20 Parkinson's disease patients. Magn Reson Imaging 2013;31:1068-73.
117. Bae YJ, Kim JM, Kim E, Lee KM, Kang SY, Park HS, Kim KJ, Kim YE, Oh ES, Yun JY, Kim JS, Jeong HJ, Jeon B, Kim SE. Loss of Nigral Hyperintensity on 3 Tesla MRI of Parkinsonism: Comparison With (123) I-FP-CIT SPECT. Mov Disord 2016;31:684-92.
118. Reiter E, Mueller C, Pinter B, Krismer F, Scherfler C, Esterhammer R, Kremser C, Schocke M, Wenning GK, Poewe W, Seppi K. Dorsolateral nigral hyperintensity on 3.0T susceptibility-weighted imaging in neurodegenerative Parkinsonism. Mov Disord 2015;30:1068-76.
119. Blazejewska AI, Schwarz ST, Pitiot A, Stephenson MC, Lowe J, Bajaj N, Bowtell RW, Auer DP, Gowland PA. Visualization of nigrosome 1 and its loss in PD: pathoanatomical correlation and in vivo 7 T MRI. Neurology 2013;81:534-40.
120. Kosta P, Argyropoulou MI, Markoula S, Konitsiotis S. MRI evaluation of the basal ganglia size and iron content in patients with Parkinson's disease. J Neurol 2006;253:26-32.
121. Huang LZ, Parameswaran N, Bordia T, Michael McIntosh J, Quik M. Nicotine is neuroprotective when administered before but not after nigrostriatal damage in rats and monkeys. J Neurochem 2009;109:826-37.

Cite this article as: Gu Q, Liu X, Zeng Q, Guan X, Zhou C, Guo T, Zhang B, Zhang M. The protective role of cigarette smoking against Parkinson's disease via moderation of the interaction between iron deposition in the nigrostriatal pathway and clinical symptoms. Quant Imaging Med Surg 2022;12(7):3603-3624. doi: 10.21037/qims-21-1090

Supplementary

Table S1 The susceptibility values (ppm) of the deep brain nuclei across groups

	Group	Numbers	Mean	SD	SE	95% CI	Range	
L_putamen	ns-HC	24	0.038	0.013	0.003	0.032-0.043	0.020	0.069
	ns-PD	17	0.038	0.012	0.003	0.032-0.044	0.010	0.059
	s-HC	23	0.037	0.014	0.003	0.031-0.043	0.016	0.070
	s-PD	18	0.032	0.013	0.003	0.025-0.038	0.011	0.069
	Total	82	0.036	0.013	0.001	0.033-0.039	0.010	0.070
L_caudate	ns-HC	24	0.028	0.008	0.002	0.025-0.031	0.016	0.045
	ns-PD	17	0.025	0.008	0.002	0.021-0.029	0.012	0.039
	s-HC	23	0.025	0.008	0.002	0.022-0.028	0.008	0.043
	s-PD	18	0.026	0.008	0.002	0.022-0.03	0.011	0.039
	Total	82	0.026	0.008	0.001	0.024-0.028	0.008	0.045
L_globus	ns-HC	24	0.078	0.031	0.006	0.065-0.091	0.018	0.169
	ns-PD	17	0.071	0.019	0.005	0.062-0.081	0.033	0.106
	s-HC	23	0.062	0.026	0.005	0.051-0.074	0.027	0.147
	s-PD	18	0.058	0.018	0.004	0.049-0.067	0.027	0.083
	Total	82	0.068	0.026	0.003	0.062-0.074	0.018	0.169
L_red nucleus	ns-HC	24	0.065	0.025	0.005	0.054-0.075	0.010	0.133
	ns-PD	17	0.078	0.021	0.005	0.067-0.089	0.058	0.116
	s-HC	23	0.059	0.018	0.004	0.051-0.067	0.031	0.099
	s-PD	18	0.065	0.019	0.005	0.056-0.075	0.030	0.099
	Total	82	0.066	0.022	0.002	0.061-0.071	0.010	0.133
L_SNc	ns-HC	24	0.040	0.022	0.004	0.031-0.049	0.011	0.090
	ns-PD	17	0.047	0.017	0.004	0.038-0.056	0.016	0.070
	s-HC	23	0.030	0.012	0.002	0.025-0.035	0.010	0.056
	s-PD	18	0.033	0.010	0.002	0.028-0.038	0.015	0.050
	Total	82	0.037	0.017	0.002	0.033-0.041	0.010	0.090
L_thalamus	ns-HC	24	0.007	0.005	0.001	0.005-0.010	-0.003	0.019
	ns-PD	17	0.006	0.005	0.001	0.003-0.008	0.000	0.020
	s-HC	23	0.005	0.007	0.001	0.002-0.008	-0.004	0.025
	s-PD	18	0.006	0.006	0.001	0.003-0.009	-0.005	0.018
	Total	82	0.006	0.006	0.001	0.005-0.007	-0.005	0.025
L_SNr	ns-HC	24	0.083	0.029	0.006	0.070-0.095	0.025	0.152
	ns-PD	17	0.088	0.023	0.006	0.076-0.100	0.046	0.123
	s-HC	23	0.076	0.017	0.003	0.069-0.084	0.039	0.111
	s-PD	18	0.080	0.027	0.006	0.067-0.093	0.033	0.146
	Total	82	0.081	0.024	0.003	0.076-0.087	0.025	0.152

Table S1 (*continued*)

https://dx.doi.org/10.21037/qims-21-1090

Table S1 (*continued*)

	Group	Numbers	Mean	SD	SE	95% CI	Range	
R_caudate	ns-HC	24	0.029	0.009	0.002	0.026-0.033	0.016	0.048
	ns-PD	17	0.025	0.009	0.002	0.021-0.030	0.009	0.043
	s-HC	23	0.028	0.008	0.002	0.025-0.031	0.012	0.043
	s-PD	18	0.025	0.009	0.002	0.021-0.030	0.013	0.051
	Total	82	0.027	0.009	0.001	0.025-0.029	0.009	0.051
R_putamen	ns-HC	24	0.038	0.014	0.003	0.032-0.043	0.016	0.064
	ns-PD	17	0.035	0.012	0.003	0.029-0.041	0.012	0.053
	s-HC	23	0.040	0.018	0.004	0.032-0.048	0.017	0.092
	s-PD	18	0.031	0.009	0.002	0.026-0.035	0.016	0.048
	Total	82	0.036	0.014	0.002	0.033-0.039	0.012	0.092
R_globus	ns-HC	24	0.079	0.029	0.006	0.067-0.091	0.017	0.170
	ns-PD	17	0.073	0.021	0.005	0.062-0.084	0.044	0.134
	s-HC	23	0.064	0.023	0.005	0.054-0.074	0.031	0.124
	s-PD	18	0.056	0.017	0.004	0.048-0.064	0.026	0.092
	Total	82	0.069	0.025	0.003	0.063-0.074	0.017	0.170
R_red nucleus	ns-HC	24	0.068	0.026	0.005	0.058-0.079	0.016	0.148
	ns-PD	17	0.078	0.019	0.005	0.068-0.088	0.054	0.125
	s-HC	23	0.063	0.021	0.004	0.054-0.072	0.014	0.103
	s-PD	18	0.067	0.018	0.004	0.058-0.076	0.028	0.096
	Total	82	0.069	0.022	0.002	0.064-0.074	0.014	0.148
R_SNc	ns-HC	24	0.040	0.022	0.004	0.03-0.049	0.015	0.105
	ns-PD	17	0.042	0.016	0.004	0.034-0.05	0.025	0.081
	s-HC	23	0.035	0.015	0.003	0.028-0.041	0.005	0.062
	s-PD	18	0.032	0.012	0.003	0.026-0.038	0.009	0.054
	Total	82	0.037	0.017	0.002	0.033-0.041	0.005	0.105
R_thalamus	ns-HC	24	0.008	0.005	0.001	0.006-0.01	-0.001	0.019
	ns-PD	17	0.006	0.005	0.001	0.004-0.008	-0.001	0.017
	s-HC	23	0.005	0.007	0.001	0.002-0.008	-0.005	0.030
	s-PD	18	0.007	0.005	0.001	0.004-0.009	0.000	0.017
	Total	82	0.006	0.006	0.001	0.005-0.008	-0.005	0.030
R_SNr	ns-HC	24	0.091	0.028	0.006	0.08-0.103	0.037	0.146
	ns-PD	17	0.090	0.025	0.006	0.077-0.103	0.044	0.133
	s-HC	23	0.080	0.017	0.004	0.072-0.087	0.049	0.115
	s-PD	18	0.073	0.022	0.005	0.062-0.084	0.038	0.122
	Total	82	0.084	0.024	0.003	0.078-0.089	0.037	0.146

SNc, substantia nigra pars compacta; SNr, substantia nigra pars reticulata.

https://dx.doi.org/10.21037/qims-21-1090

Table S2 The regions of interest (ROIs) with significant differences in QSM values (ppm) across groups (controlling for disease duration, age and TIV)

	Main effect		Pairwise comparison					
	Group		Group I-J	Mean Diff (I-J)	SE	P' (*)	95% CI	
	F	P (*)					Lower	Upper
R_GP	3.973	0.011*	ns-HC – ns-PD	0.013	0.01	1.000	-0.015	0.04
			ns-HC – s-HC	0.015	0.007	0.217	-0.004	0.033
			ns-HC – s-PD	0.028	0.009	0.016*	0.004	0.052
			ns-PD – s-HC	0.002	0.01	1.000	-0.026	0.03
			ns-PD – s-PD	0.015	0.008	0.437	-0.007	0.037
			s-HC – s-PD	0.013	0.009	0.92	-0.011	0.037

Multiple pairwise comparisons were corrected by Bonferroni method, with a pre-adjusted significance (*) level at P'<0.05. GP, globus pallidum; I-J means the two groups for comparison; SE, standard error; CI, confidence interval.

Table S3 Two-way MANCOVA and pairwise comparisons in QSM values (ppm) across groups (controlling for disease duration, age and TIV)

Source		Mean square	F	Partial eta square	Pairwise comparison					
					Group I>J	Mean Diff (I–J)	SE	P' (*)	95% CI	
									Lower	Upper
Smoking status	R_GP	0.004	7.631	0.092	Non-smokers > smokers	0.015	0.005	0.007*	0.004	0.025
	L_GP	0.004	6.746	0.083		0.015	0.006	0.011*	0.003	0.026
	R_SNc	0.001	4.649	0.058		0.008	0.004	0.034*	0.001	0.016
	L_SNc	0.003	10.046	0.118		0.012	0.004	0.002*	0.004	0.019
	R_SNr	0.005	10.046	0.118		0.015	0.005	0.002*	0.006	0.025

The threshold of pre-adjusted significance (*) was regarded as P'<0.05 corrected by Bonferroni method. GP, globus pallidum; RN, red nucleus; SNc, substantia nigra compacta; SNr, substantia nigra pars reticulata.

https://dx.doi.org/10.21037/qims-21-1090

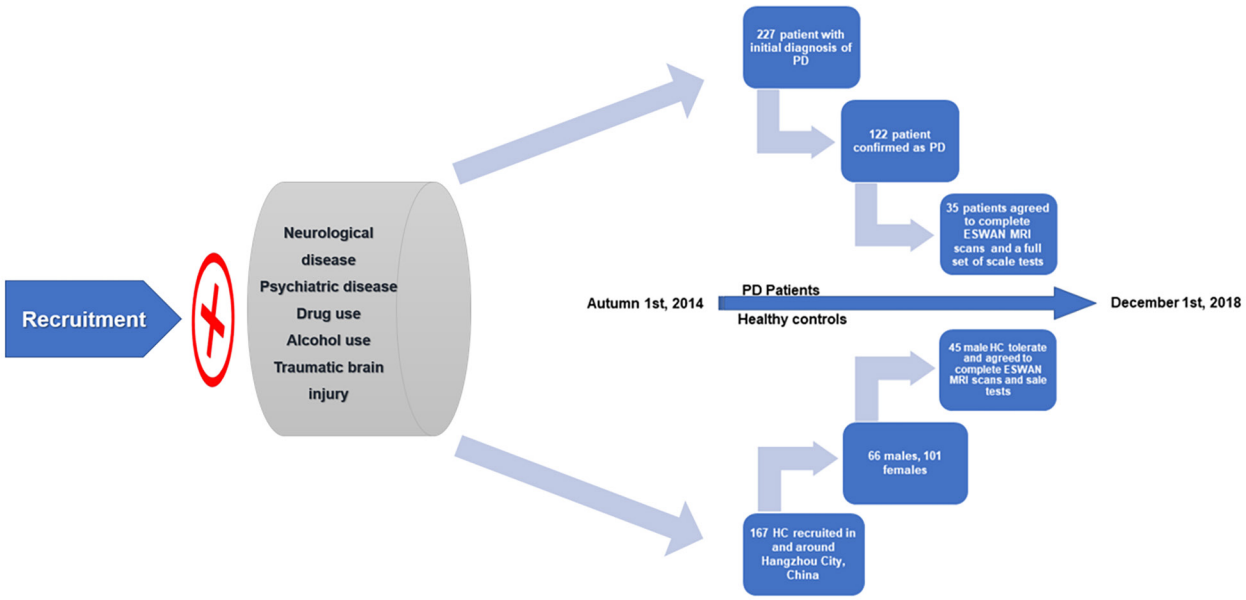

Figure S1 The flow chart of the recruitment of Parkinson's disease (PD) patients.

https://dx.doi.org/10.21037/qims-21-1090

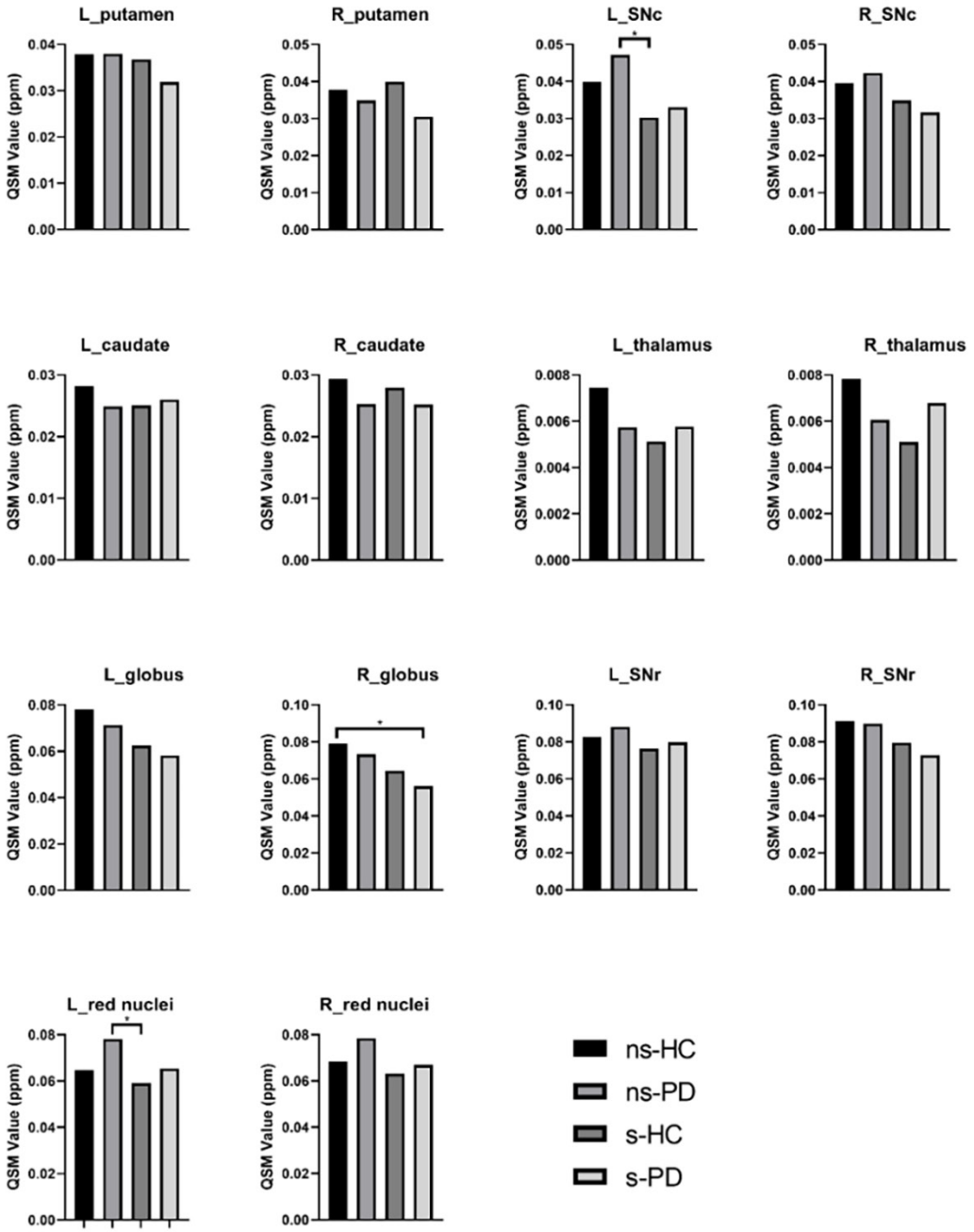

Figure S2 The ROIs with significant differences in QSM values (ppm) across groups. *, the significance level was at P<0.05. SNc, substantia nigra pars compacta; SNr, substantia nigra pars reticulata.

https://dx.doi.org/10.21037/qims-21-1090